TESIS

Universidad de Jaén

Campus Científico Tecnológico de Linares

ESTUDIO EXPERIMENTAL Y NUMÉRICO SOBRE LAS PRESTACIONES DE UN SISTEMA TÉRMICO FOTOVOLTAICO CONECTADO EN SERIE A UN SISTEMA SOLAR TÉRMICO

Autor: Hayder Altharwanee

Director de la tesis: Francisco Jurado Melguizo and David Vera Candeas

Departamento: Electrical Engineering

Fecha: XX/XX/XXXX

ISBN:

RUJA

TESIS

Universidad de Jaén

Linares Scientific and Technological Campus

PERFORMANCE EVALUATION OF AN INTEGRATED PVT–SOLAR THERMAL SYSTEM: EXPERIMENTAL AND NUMERICAL APPROACH

Author: Hayder Altharwanee

Thesis director: Francisco Jurado Melguizo and David Vera Candeas

Department: Electrical Engineering

Acknowledgments

I would like to express my profound thankfulness and heartfelt gratitude to every individual and organization that has contributed to my personal and academic achievements throughout my educational journey. The completion of this PhD thesis represents a significant milestone in my life, one that could not have been accomplished without the support, encouragement, and guidance of many people who have stood by me along the way. First and foremost, I am deeply indebted to my cherished wife — my most steadfast companion, confidante, and life partner. Her unwavering belief in my abilities, her boundless patience, and her constant moral support have sustained me through every challenge and triumph. From the earliest days of this scientific pursuit, she has played an essential role — providing emotional strength, taking care of our family, and encouraging me to persevere even in the most demanding times. Her presence has been a pillar of strength, and I will always be grateful for her sacrifices and dedication, without which this accomplishment would have remained a distant dream. I am also incredibly thankful to my thesis supervisors, **Professor Francisco Jurado Melguizo** and **Professor David Vera**, whose guidance, mentorship, and expertise have played a pivotal role in the development and success of this research. Their unwavering support, valuable insights, and constructive feedback have helped shape this work from its inception to completion. I am particularly grateful to **Professor Francisco Jurado**, whose extensive knowledge, thoughtful suggestions, and constant encouragement have been of immeasurable value. Equally, I would like to sincerely thank **Professor David Vera** for his kind cooperation, technical assistance, and collaborative spirit throughout the course of this study. Their dedication to excellence and commitment to supporting their students have left a lasting impression on me, and I consider myself fortunate to have worked under their supervision. Without their generous support and guidance, this research would not have reached its full potential. I would also like to extend my sincere appreciation to the **Electrical Engineering Department at the University of Jaén, Linares College**, for providing me with all the essential facilities, research tools, and a conducive academic environment necessary for carrying out this work. The department's commitment to research and innovation greatly contributed to the successful realization of this thesis. My deepest thanks also go to the **local administration of the Holy Karbala Governorate** for their financial support, which significantly aided in the completion of my academic pursuits. Their backing has been instrumental in facilitating my progress and allowing me to focus on my research without undue hardship. Furthermore, I would like to acknowledge all my colleagues, friends, and fellow researchers who have supported me directly or indirectly during this journey. Whether through thoughtful discussions, encouragement, collaboration, or simply being a source of motivation, their contribution has not gone unnoticed. Every word of encouragement, every shared idea, and every gesture of kindness has helped shape this journey into one of growth and discovery. Lastly — but most importantly — I wish to extend my deepest gratitude to my entire family. Their love, prayers, and unshakeable support have guided me through every stage of my academic and personal life.

This thesis is not only a reflection of my academic efforts but also a tribute to all those who stood beside me with unwavering support and belief. Thank you all, from the depths of my heart.

<u>Brief overview</u>

in 150 words

The present study is designed to enhance the thermal efficacy of the solar thermal collector (ST) system by integrating it with the photovoltaic thermal (PVT) system. Furthermore, it entails the demonstration of the integrated system's ability to heat a specific room and satisfy the demand for hot water. Experimental and numerical simulation analyses of the integrated system are conducted under four distinct days, months, and environmental conditions. Alongside the thermal energy advantages of the utilized system, the system includes electricity generation from the PVT system.

The whole system has enough potential energy to sufficiently heat a sizable fraction of a single room and also satisfy a major share of the small home hot water demand. For a small family, this system offers a sustainable energy source that might account as a good share of the thermal and electrical demand.

<u>Breve resumen</u>

en 150 palabras

Este estudio se enfoca en la integración del recolector solar térmico (ST) con el sistema fotovoltaico térmico (PVT), con el objetivo de optimizar la eficiencia térmica del sistema ST. Adicionalmente, conlleva poner de manifiesto la habilidad del sistema integrado para cumplir con la demanda de agua caliente y para calentar una única estancia. El estudio abarca estudios de simulación numérica y experimental de la estructura del sistema durante un período de cuatro días en meses distintos y a través de diversas condiciones ambientales. El sistema de investigación comprende la producción eléctrica a través del sistema PVT, junto con las ventajas térmicas intrínsecas al conjunto. El sistema integral posee la capacidad energética necesaria para calentar de manera adecuada una porción considerable de una habitación, Además de satisfacer una considerable proporción de las necesidades de agua caliente en un hogar de dimensiones limitadas. Este sistema constituye una fuente de energía sostenible que podría proporcionar una porción significativa de la energía termal y eléctrica requerida para una familia de menor tamaño.

Abstract

This study introduces an experimental method for integrating photovoltaic thermal (PVT) and solar thermal (ST) collectors as a hybrid PVT-ST (PVTST) system, with the goal of improving both thermal and electrical energy production. The performance of the system was evaluated over four consecutive days in January, February, March, and April under different weather conditions. The findings reveal that the combined PVTST system produced higher water temperatures than the individual ST system, showing increases of about 6.15°C, 6.65°C, 7.51°C, and 5.48°C on the respective days. Regarding thermal performance, the hybrid system demonstrated average efficiency improvements of 24.8%, 18.2%, 22.3%, and 19.4% compared to the ST system. The combined system's exergy efficiency increased with an average of (7.98, 7.45, 7.82, and 6.97) %, respectively, compared to the same collector.

The PVT system resulted in a significant increase in electrical efficiency, with average improvements of 31.04%, 41.16%, 47.34%, and 11.55% in comparison to a standard photovoltaic (PV) panel on the four days that were observed. The combined system and standalone ST system were both effective in sustaining comfortable indoor temperatures of a single room during February, March, and April, as further confirmed by the simulation results. Nevertheless, the ST system encountered a heating deficit of approximately 15.9% in January, while the PVTST system experienced a lesser deficit of approximately 8.18%. Furthermore, the combined system was capable of meeting approximately 61.4%, 79.4%, 77.3%, and 75% of the total hot water demand on the respective test days, as indicated by the performance evaluations.

Resumen

La combinación de un sistema fotovoltaico térmico (PVT) con un sistema solar térmico (ST) permite simultáneamente lograr dos metas: la primera es la obtención de energía térmica y la optimización de su eficiencia, la segunda es la obtención de energía eléctrica y la optimización de su eficiencia. Este estudio constituye una investigación experimental que integra los sistemas PVT y ST (PVTST) para evaluar su rendimiento bajo diversas condiciones climáticas en cuatro días separados en enero, febrero, marzo y abril. Los resultados revelaron que el sistema PVTST aumentó la temperatura del agua caliente de salida en mayor medida que el sistema ST por sí solo. En los cuatro días de pruebas, la temperatura de salida del PVTST aumentó aproximadamente 6,15, 6,65, 7,51 y 5,48 °C, respectivamente, más que la temperatura del sistema ST. Durante los cuatro días de prueba, la eficacia térmica del sistema PVTST mejoró en promedio un 24,8%, 18,2%, 22,3% y 19,4% en comparación con el sistema ST. La eficiencia de la exergía del sistema combinado mejoró en un promedio de 7,98%, 7,45%, 7,82% y 6,97%, respectivamente.

Durante los cuatro días seleccionados, la eficiencia eléctrica media mejoró un 31,04%, 41,16%, 47,34% y 11,55%, respectivamente, en comparación con el panel fotovoltaico convencional cuando se empleó un sistema PVT. Los resultados de la simulación del calentamiento de una sola habitación indican que tanto el PVTST como el ST pueden calentar eficazmente una sola habitación durante el período de prueba de febrero, marzo y abril. Por otra parte, en enero el déficit del sistema ST se situaba en torno al 15,9%, y el déficit del sistema PVTST en torno al 8,18%. Los resultados demuestran que el sistema PVTST actual tiene la capacidad de atender aproximadamente el 61,4%, 79,4%, 77,3% y 75% de la demanda necesaria de temperatura de agua caliente en los días considerados.

Abbreviations

D_h	hydraulic diameter
G	solar radiation
U	average velocity
$m^{\cdot}$	mass flow rate
k	thermal conductivity
h_c	convection heat transfer coefficient
k	turbulence kinetic energy (for the turbulent model)
I	heat source radiation
u_i, u_j	velocity vectors of i and j, respectively
x_i, x_j	position vectors of i and j, respectively
P_o	outlet pressure
T	temperature
A	collector surface area
Cp	constant pressure heat capacity
L	characteristic length
Q_c, Q_{rad}	convection and radiation heat transfer rate, respectively
Re	Reynolds number
T_a, T_r	ambient and average room temperatures, respectively
T_g, T_{sky}	glass and sky temperatures, respectively
T_i, T_o	inlet and outlet temperatures, respectively
T_{pv}, T_{ref}	PV surface temperature and reference temperature, respectively
Gr	Grashof number
V_f	fluid velocity
Pr	Prandtl number

G_b, G_k turbulence kinetic energy generation of buoyancy and velocity gradient, respectively.

Y_M dilatation dissipation

Greek symbols:

ε turbulence dissipation rate

ϱ fluid density

α_k, α_ε inverse of Prandtl number for k and ε, respectively

S_k, S_ϵ source terms

R_ϵ streamline curvature

ζ exergy efficiency

η thermal efficiency

μ solar cell temp. coefficient (for the electrical efficiency equation)

ν, μ kinematic viscosity and viscosity, respectively

σ, σ_s Steven Boltzmann and coefficient of scattering, respectively

Ω' solid angle

φ phase function

μ_{eff} effective viscosity

β thermal expansion coefficient

$C_{1\varepsilon}$, $C_{2\varepsilon}$, $C_{3\varepsilon}$ constants

Subscriptions:

ST flat plate solar collector

PVT photovoltaic thermal collector

PVTST the combined system of PVT&ST

Table of Contents

List of Figures

List of Tables

Chapter 1

Introduction

1.0.1 Global warming

Global warming signifies a rise in global temperatures affecting the atmosphere's lower levels [3]. This phenomenon is also known as "climate change." The sun generally warms our planet by its radiation, regarding some of it being reflected back into the atmosphere. Nevertheless, carbon dioxide and other greenhouse gases absorb and then reflect this energy toward the Earth's surface, resulting in global warming. In this way, it poses an imminent threat to our planet as we understand it. It is projected that the economy, human health, and natural ecosystems will be significantly impacted by global warming issues. It is anticipated that climate change will disrupt ecosystems and lead to a reduction in species diversity, as numerous species will be unable to adjust to the fast-shifting environmental circumstances. If we don't tackle global warming with current technology, we will ultimately be unable to sustain both the global population and our quality of living [4].

1.0.2 Net zero emissions and Paris agreement

As mentioned, recently, climate change is an essential concern, prompting 195 nations to endorse the Paris agreement and pledge to restrict global warming to below 2°C relative to the beginning of industrialization [5]. The term "net zero" denotes the equilibrium between the quantity of greenhouse gases (GHGs) that are generated and the quantity that is eliminated from the atmosphere. The NZE procedure can be seen in figure 1.1, where it's predicted that NZE will be achieved by 2050. It can be accomplished by employing a combination of emission reduction and emission removal. Selecting the most suitable renewable energy sources can help one to get net emissions of zero greenhouse gas [6]. In the NZE plan, wind and solar expansion are the primary factors times increase by 2050 in the NZE. The global contribution of clean energy sources in total power production increased from 29% in 2020 to more than 60% in 2030 and to almost 90 percent in 2050 [7]. Available renewable energy sources are essential for ensuring electrical security, alongside alternative low-carbon production sources, robust power storage, and electricity supply networks. Renewable energy sources substantially reduce emissions in buildings, industry, and transportation. contributing to the tripling of renewable energy generation by 2030. Renewables can be utilized either indirectly, through the

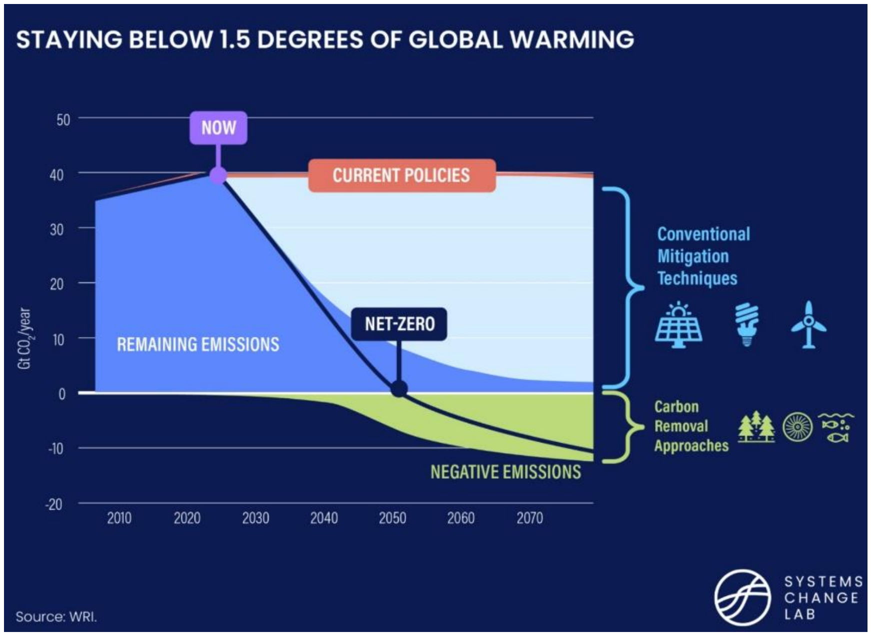

Figure 1.1: Net zero emission target [1]

utilization of electrical energy or thermal energy generated from renewable sources, or directly, primarily for heat production. Figure 1.2 shows the energy sources share from 2010 until 2050 in the mentioned sectors [7]. For electricity generation sector, by 2030 its supposed as its programmed, the direct renewable energy will be 61%, while other low-carbon sources and fossil sources are 14% and 25%, respectively. By 2050 these percents will be 88%, 12%, and 0%, for the renewable energy, low-carbon, and fossil fuel sources, respectively. In transportation sector, renewable energy significantly contributes to pollution reduction by generating electricity for electric vehicles. They also facilitate direct reductions in emissions via the utilization of liquid biofuels and biomethane. By 2030, its programmed that the direct and indirect renewable energy will share 16%, and the other low-carbon sources and fossil sources will be approximately, 3% and 81%, respectively. while these values by 2050 will be 61%, 30%, and 10% for the renewable energy, low-carbon, and fossil sources, respectively. For the building sector, by 2030, it's programmed that the direct and indirect renewable energy will share 37%, and the other low-carbon sources and fossil sources will be 5% and 58%, respectively. While these values by 2050 will be 81%, 11%, and 9% for the renewable energy, low- carbon, and fossil sources, respectively. Based to [7], the direct usage of renewable energy is predicted to rise to 40% by 2025, same figure shows. Whenever feasible, renewables are paired with deep

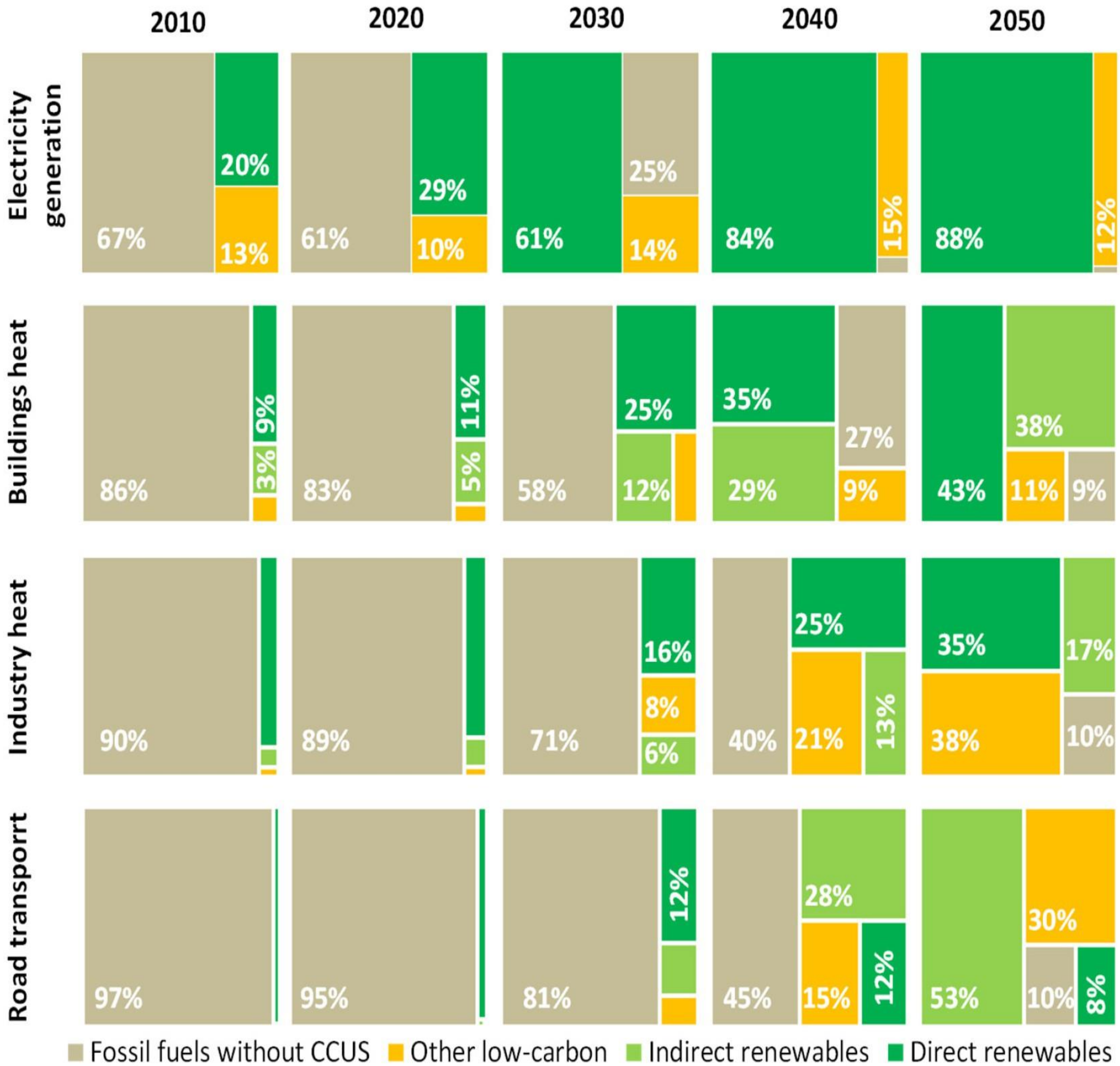

Figure 1.2: Energy share prediction of different sectors from 2010 to 2050 [2]

retrofits and energy-related building codes. By 2050, solar thermal water heaters will be installed in nearly all buildings through located roof area and suitable amount of solar radiation. This is due to fact that heating energy in water tanks is usually more affordable than electricity storage and they are less costly per square meter than solar PV. It is anticipated that by 2030, there will be 100 million rooftops thermal water collectors, and by 2050, there will be 240 million. Rooftop solar PV generates renewable electricity on-site. In the industrial sector, by 2030, its programmed that the direct and indirect renewable energy will share 22%, and the other low-carbon sources and fossil sources will be 8% and 71%, respectively. while these values by 2050 will be 52%, 38%, and 10% for the renewable energy, low-carbon, and fossil sources, respectively. In the NZE plan, bioenergy is the main direct energy from renewable sources for low- and medium-temperature requirements. Low-temperature heat produced by solar thermal and geothermal sources has application in non-energy-intensive sectors as well as in auxiliary activities in heavy industry. By 2030, bioenergy, solar thermal, and geothermal sources are projected to fulfill approximately 15% of industrial heat demand, approximately double their 2010 contribution, growing to 40% by 2050. The not direct use of renewable sources of energy via electrical power will increase the share of renewables in total industrial energy consumption by 15% by 2050.

1.1 Renewable energy

As global energy consumption escalates and the detrimental effects of fossil fuels on the environment become more and more clear, the imperative for sustainable and renewable energy sources has intensified. It is essential to reduce the reliance on fossil fuels in the energy structure today's civilization, as heat and electricity production predominantly relies on combustion techniques that adversely impact the environment and contribute to global warming. As depicted in Fig. 1.3 [2], global energy use is projected to continue growing significantly by 2050.

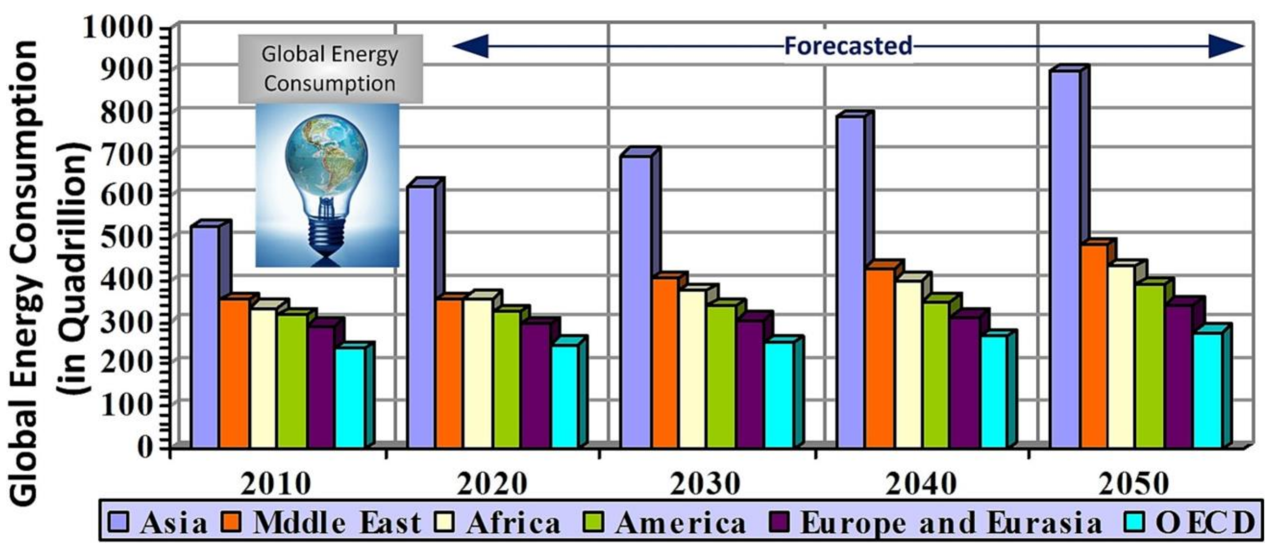

Figure 1.3: Energy consumption prediction from 2010 to 2050[2]

Renewable energy has been seen as an adequate answer to the emission issue and the energy demand in recent years [14]. Renewable energy is a type of energy that uses natural resources that are continually regenerated rather than diminished. Renewable energy is predicted to make over 67% of world energy consumption by 2050. Wind energy and solar energy will be the majority of the renewable energy sources, accounting for 24% and 19% of total power generation by 2050, respectively [15].

Experts expect that energy usage would rise by 1.5 to 3 times by 2050 [16]. Solar energy is the most accessible, cost-effective, and environmentally safe among the others renewable energy sources. It has considerable potential to significantly contribute to the change to sustainable and renewable sources of energy. In the building field, solar energy is crucial for lowering carbon emissions and energy use. Almost all of Earth's energy comes from indirect solar energy [17]. The International Energy Agency (IEA) report for 2023 (energy efficiency 2023) claims that building energy cons-

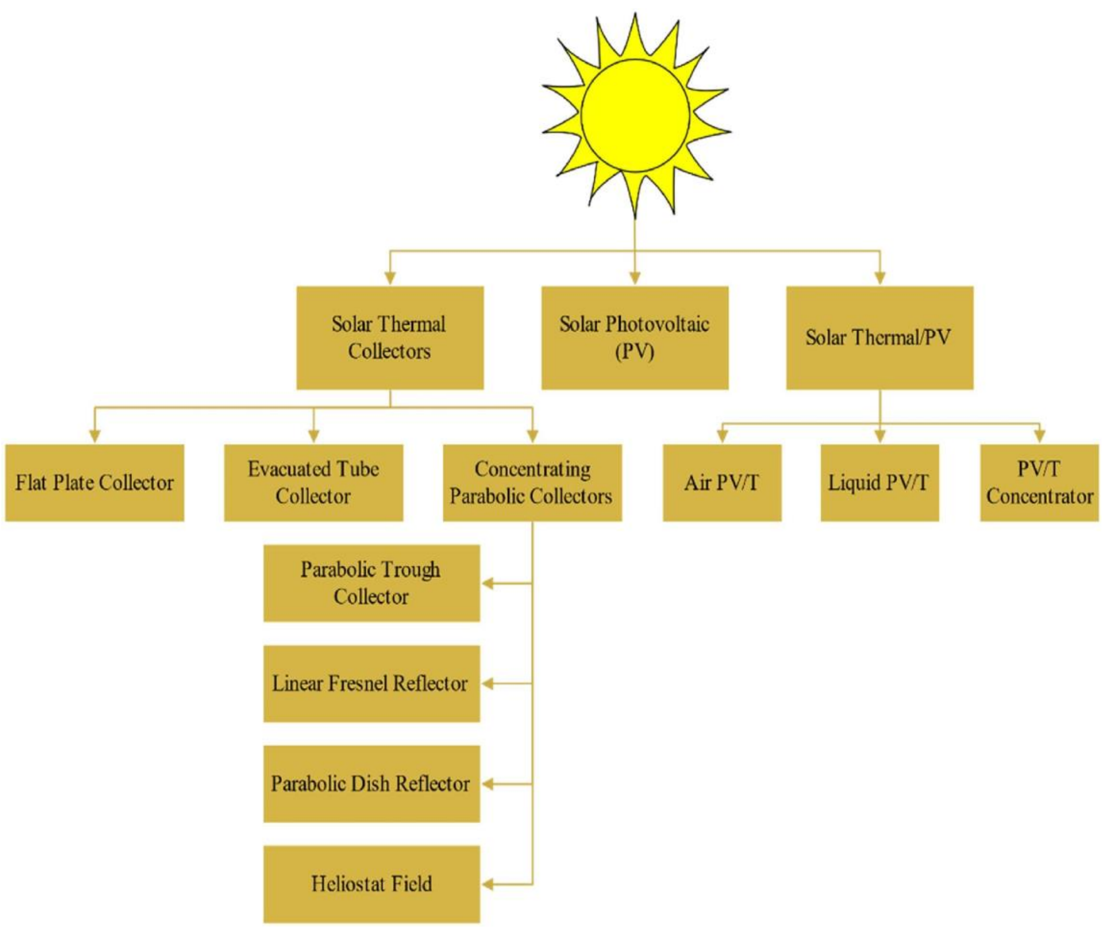

Figure 1.4: solar energy in building classification

mption accounted for 30% of the global final energy demand in 2022 [18] and 26% of emissions. The applications of solar energy buildings can be categorized primarily as photovoltaic, photovoltaic thermal systems, and solar thermal systems, as illustrated in Figure 1.4 [19]. Solar photovoltaic systems are expected to account for approximately 69.6% of the electricity output by 2030 [20]. PV systems directly transform solar into electrical energy, exhibiting low efficiency as a substantial fraction of sunlight is transformed into thermal energy. It can be said that about 80% of the sun's energy is either absorbed by PV cells or released into the environment. Thus, determining the minimum working temperature of the PV energy is essential to enhance its efficiency [21]. For this reason, the concept of photovoltaic thermal (PVT) systems has been introduced. PVT systems can achieve two benefits at the same time: the first is represented by PV cooling and limiting the excessive temperature of the PV by converting it to heat energy, and this can be employed for a variety of applications, and the second is producing electrical energy. Numerous works, numerical and experimental, have been done in this field. PVT systems offer enhanced energy production relative to traditional solar panels and can be financially feasible if the additional expense of the thermal component is limited [22]. These systems are generally categorized based on the working fluid as: water, air, and bifluid PVT based. Figure 2 shows a summary of the standard PVT systems types and the new or improved PVT systems beside the other types of solar energy [23].

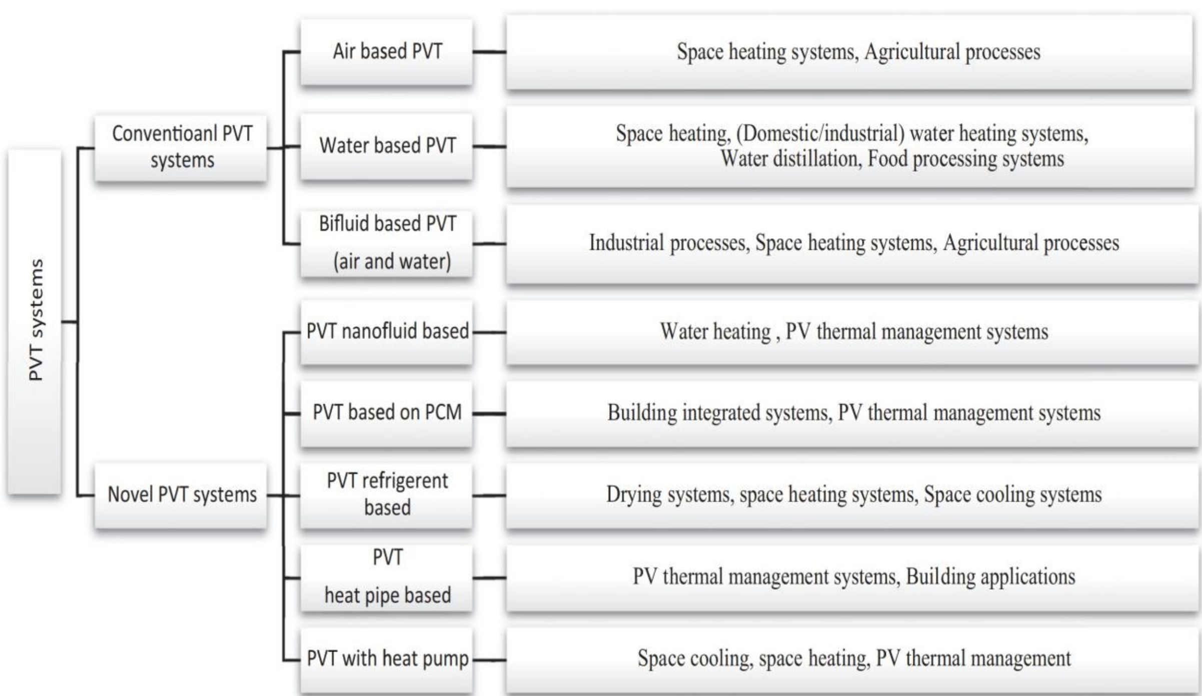

Figure 1.5: PVT systems classification

This technology has the potential to be implemented in buildings, particularly where its installation space is impacted [24]. Water heating, domestic or industrial space heating, space cooling, water distillation, food processing, agricultural processes, thermal management systems of PV panels, integrated building systems, and drying systems are the most PVT applications [23].

The European PVT Roadmap (2005) found that the single-cover PVT collector utilizing liquid as a heat transfer fluid is the primary market product for PVT collectors, primarily used for water heating and space heating applications [25]. The previous figure (1.4) illustrates that solar thermal collectors can be categorized into flat plate solar thermal collectors, evacuated tube collectors, and concentrating parabolic collectors. The main purposes of these devices involve converting solar energy into thermal energy. They can perform a variety of functions, although they are generally used to heat the space or make hot water [26]. With regard to the various kinds of these collectors, the flat plate solar collector is the most cost-effective and simple to operate. The assembly mainly involves the following materials: a transparent cover, an absorber body, pipes, insulation, and a backplate.

A flat surface receives as much solar radiation as possible and then converts it into heat energy. Thermal energy is captured by the heat transfer fluid that flows beneath the absorber through convection and conduction and is subsequently stored for the future use. The thermal effectiveness of this collector type is poor, especially in colder seasons. During the winter season, the solar collector's efficiency drops from 75% during the summer season to as low as 40% [27]. Numerous studies have been focused on the thermal efficiency of PVT and flat plate collectors. Researchers utilized passive and active methods to enhance thermal performance. Passive methods don't need external forces, while active methods do. Ribs [28], baffles [29],grooves [30], extending surfaces using fins [31], porous [32], twisted tape [33], phase change material (PCM) [34], vortex generator [35], and nanofluid [36] represent cases of passive techniques employed to optimize the energy efficiency of these collectors.

PVT systems combined to solar thermal (ST) systems have been the subject of a few recent studies. This technique can be known as PVTST, and the main objectives of these studies represent increasing the output temperature of the ST systems and generate electricity while simultaneously resolving the PVT systems' output temperature shortfall. The current thesis investigates experimentally the thermal performance of the PVT system combined to the ST system under various environmental conditions; additionally, this thesis investigates numerically the

PVTST behavior by coupling it to the space heating system, as will be demonstrated in the following sessions.

1.2 The study objectives

The current thesis, as clarified before, monitors in the thermal performance of a PVT system coupled in series to a ST system under four different climatic conditions covering four days during four months. The primary goals of the present investigation can be summarized as follows:

1- Improving the ST system thermal performance.

2- Introducing a literature review of the recent studies that have been done in the area of the PVTST systems.

3- Enhancing the total electrical efficiency of the photovoltaic system.

4- Modeling and simulation of specific space heating.

5- Showing the PVTST system capabilities, whether it can meet the room space heating.

6- Evaluating the inadequacy of hot water produced by the system.

1.3 Thesis structure

The thesis commences with an introductory chapter that outlines the research framework, objectives, and the significance of the study. This is succeeded by a Literature Review chapter, which examines prior research and theoretical foundations to establish the context and rationale for the current investigation. The Methodology chapter details the research design, experimental tools, data collection approaches, and analytical methods employed to address the research questions. In the Results chapter, the key findings are presented, which are then thoroughly analyzed and interpreted, emphasizing their practical implications and relevance. The thesis concludes with a Conclusion chapter that synthesizes the primary findings, assesses their importance, and provides suggestions for further research directions.

1.4 working method

The present study is structured into two primary sections, each addressing distinct yet interconnected aspects of the research. The first section provides a comprehensive overview of the testing methodologies and the ambient conditions under which the experiments were conducted. This segment delves into the specifics of the equipment, materials, experimental setup, time intervals, and all relevant tools utilized during the investigation. Furthermore, the incorporation of a numerical model, along with its verification and validation processes, is emphasized to ensure the accuracy and reliability of the experimental outcomes. A key focus of this section is to highlight the thermal and electrical performance of the system, alongside other critical parameters that contribute to the overall findings of the study. The second section of the research is dedicated to the modeling and simulation of a single room's heating process, leveraging the results derived from the first section. The primary aim of this simulation is to illustrate the system's capabilities and effectiveness in different scenarios. To achieve this, a detailed model is constructed, which is subsequently verified and validated by comparing its outputs with the available experimental data. This step is crucial to confirm the model's accuracy and to ensure that it reliably represents the real behavior of the system. Together, these two sections provide a thorough and well-rounded exploration of the system's performance, combining experimental rigor with computational analysis to deliver meaningful insights for the current thesis objects.

Expected results

The combination of the solar thermal (ST) system with the photovoltaic-thermal (PVT) system is projected to elevate the temperature of the water exiting the ST system. This increase in temperature enhances both the thermal and exergy efficiencies of the integrated system. Furthermore, the PVT system is engineered to boost thermal efficiency by transferring excess heat from the photovoltaic (PV) panels via a heat exchanger mounted on the back of the PV modules.

This mechanism is expected to reduce the surface temperature of the PV panels, thereby improving their electrical efficiency. It's expected that, the integrated system exhibits significant energy potential, enabling it to heat a substantial area of a single room and provide adequate domestic hot water (DHW) for a small household. It is important to note that domestic hot water consumption represents about 25% of the total energy used in residential settings [37]. This highlights the critical role of optimizing such hybrid systems to minimize energy consumption and enhance overall efficiency in homes. By harnessing the combined benefits of the ST and PVT systems, this integrated approach presents a viable solution for promoting sustainable energy practices in residential environments.

Chapter 2

Recent studies

2.1 Introduction

A review of literature offers a comprehensive review of the current research and different ideas relevant to the subject of this study. This section lays the framework for the research concerns and objectives through a critical analysis of pertinent studies. Moreover, it underscores the contributions of prior studies while recognizing limitations and avenues for further inquiry, ensuring that this study is both informed by and contributes to the continuing academic discourse. PVT and ST systems play a significant role in cogeneration and polygeneration systems. The cogeneration system is a method for simultaneously generating heat and electricity, resulting in significant energy savings. It is often related to the combustion of fossil fuels but may also be conducted utilizing some renewable energy sources and through waste burning. Recently, the tendency has shifted towards utilizing cleaner fuels for cogeneration, such as natural gas [38]. A polygeneration system is an enhanced form of a cogeneration system that simultaneously achieves many objectives, such as the generation of heat, electricity, cooling, and the production of energy or fuels [39].

In this context, the present literature review of the thesis is categorized into four sections: the first belongs to the PVT integrated or cogeneration and polygeneration

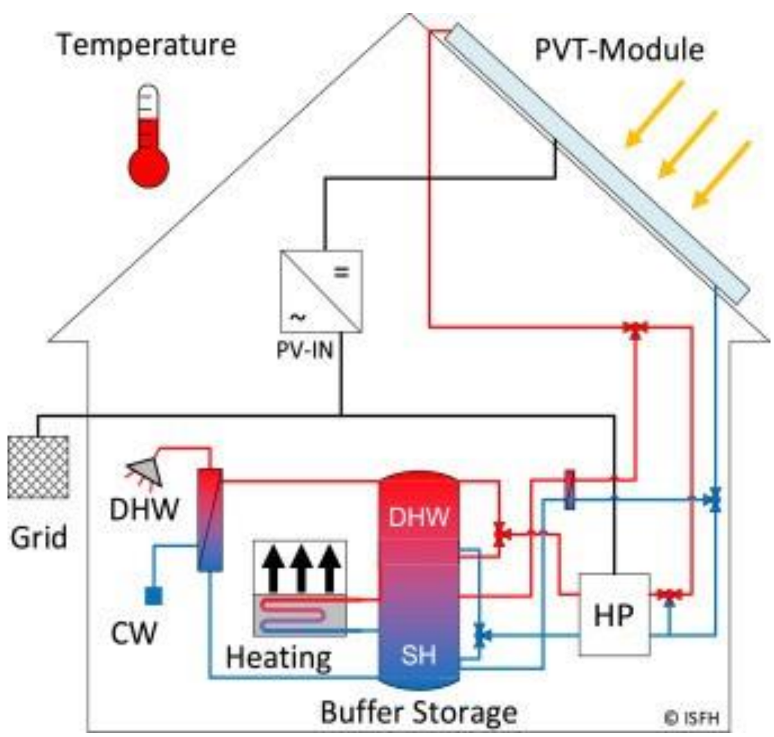

Figure 2.1: PVT-HP system schematic

systems, while the second addresses the literature review of the ST integrated or cogeneration and polygeneration systems. The third segment presents a literature review of the PVTST systems, while the fourth section entails the literature review of the PVT and ST systems applications. They might be described as follows:

2.2 PVT integrated literature review

The idea of the PVT systems was first presented in 1976 [40]. This method has grown and changed over the years and is still used presently. A lot of researchers and investigators are engaged in standard PVT systems, while some are inventing innovative methodologies [23]. Researchers have combined PVT systems with supplementary appliances or technologies to enhance thermal performance and facilitate heating, cooling, and residential hot water applications, in addition to generating electricity. Chhugani et al. [41] conducted a comparative study utilizing several types of heat source supply systems for a single-family residence. The primary focus of their investigation was on the combination of heat pump (HP) system and PVT system. In comparison to a heat pump with air source by itself, the results showed that a PVT-HP system with a 30 m^2 PVT can achieve greater performance. Furthermore, it was shown that a ground-source heat pump that is connected with a PVT system can lower the size of the heat pump by around 30–35% without having any negative effects on the efficiency of the system. Figure 2.1 illustrates the PVT-HP system schematic of their study.

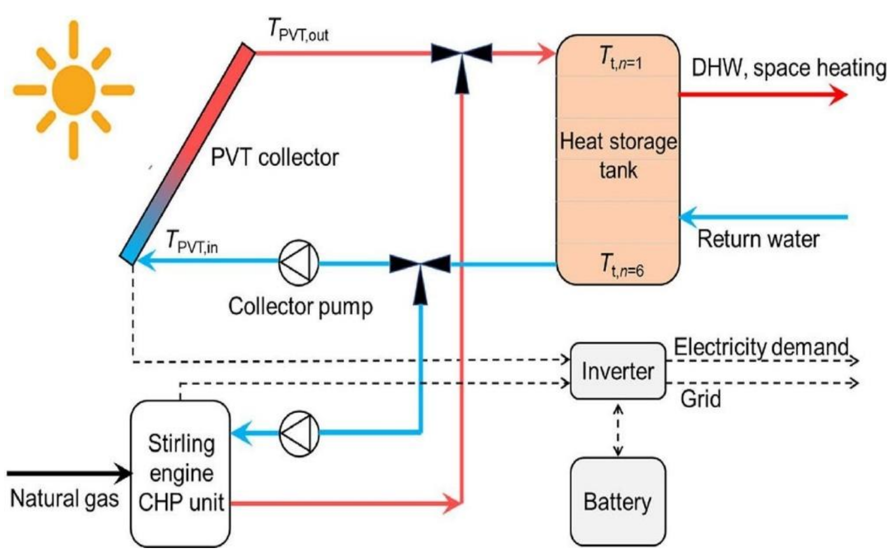

Figure 2.2: Stirling-PVT system schematic

A PVT system couples with a water source heat pump (PVT-WSHP) was conducted by Qu [42] to evaluate the impact of using this system. Their system was used as a water heating device supplies the home with hot water. In comparison to a PV-ASHP system, the results showed a 25.3% improvement in electrical performance and a decrease in yearly exergy loss. A lot of studies have been done about integrating heat and power systems by combining PVT systems and Stirling engines. Zhu [43] performed an investigation to examine the integration of 29.5 m^2 of the PVT system with a 1 KW_e Stirling engine. The integrated system reportedly attains a yearly electricity independence of 87% and fulfills 99% of the annual thermal energy requirement. Furthermore, it can attain a yearly primary energy savings rate of 35% and a carbon dioxide reduction rate of 37% relative to the reference system. See figure 2.2. Using a parabolic concentrator (CPC) and a PVT system, Tripathi and Tiwari [44] carried out an analytical study on the integration of the two systems. Their study involved a comparative analysis of the energy and exergy of four distinct systems: PVT-CPC systems, PVT systems, CPC systems, and flat plate collector systems. Two types of fluids were utilized throughout their study: water and molten salt. The results indicated that, utilizing molten salt, the PVT-CPC system and the conventional CPC system were the most appropriate for steam cooking. The PVT system can also be integrated with thermoelectric generators (TEG) to improve thermal efficiency and generate additional power simultaneously. The TEG is capable of generating electricity from the temperature difference. The PVT-TEG systems have been the subject of the labor of numerous researchers [45] [46] [47].Salari and his team[48] proposed a three-
dimensional model to analyze the system efficacy utilizing PVT/thermoelectric (TE). The performance of the PVT and PVT/TE systems was assessed by evaluating operat ional parameters including solar radiation, cooling fluid flow rate, inlet, and ambien t temperature. According to the results, the PVT/TE system's electrical performance surpasses that of the PVT system by 6.23% and 10.41% at incident solar radiation levels of 600 and 1000 W/m2, correspondingly. Additionally, the electrical efficacy of the PVT/TE increases by 0.82% as the environmental temperature increases from (26 - to 34) °C, meanwhile the PVT system exhibits a 1.4% decline. The findings of the simulation indicate that the overall electrical performance of the PVT/TE system is much higher than that of the PVT system.

2.3 ST integrated literature review

One of the most prominent examples of solar thermal energy conversion devices is the solar thermal flat plate collector, referred to as the ST in the current thesis. Its overall low efficiency results from the low thermal conductivity fluids' use [49]. However, researchers have obtained good results by integrating ST systems in cogeneration or polygeneration systems. A hybrid system consisting of 5960 m^2 of ST collector and 4039 m^2 of parabolic trough collectors was optimized by Tian et al. [50] so that they could conduct optimization studies using TRNSYS-GenOpt. The actual model has been constructed and served as a reference to validate the simulation study. The results of their investigation revealed that the integration of solar thermal collectors in the region network under investigation can reduce the heating cost by (5–9) %. F. Rosales-Pérez [51] performed an analysis and economic assessment on a hybrid system comprising a parabolic trough with flat plate collector, and an auxiliary fossil fuel system for district heating applications. Their study encompassed three distinct methods for integrating the system components. They utilized TRNSYS to conduct the comprehensive numerical simulation of their research. Using around half of the flat plate collectors, the hybrid system was able to reach a monthly solar percentage up to 91% higher than that of the standalone flat plate collector. Furthermore, the hybrid system has been attained the lowest cost among stand-alone parabolic or flat plate collectors. Algarni et al. [52] evaluated experimentally the thermal effectiveness of a hybrid system consisting of TEG and ST collector system. The investigation was conducted for three months in a cold environment. They stated that the TEG system effectively utilized the collector waste heat and thereby increasing its thermal efficacy of the collector. The findings indicated an enhancement in thermal and exergy productivity of 8.4% and 1.3%, respectively. The use of flat plate collectors as auxiliary systems in polygeneration systems has been examined in a variety of ways. These systems have been integrated with other renewable energy sources such as wind turbines, geothermal, biomass, and fuel cell energy systems as well as fossil energy sources [53] [54] [55], [56] [57] [58]. In their study, Buonomano and his group [55] conducted an optimization study that utilized trigeneration of Organic Rankine Cycle machine, ST collectors, geothermal energy and extra auxiliary devices. Their finding revealed that the system can generate cooling and heating energy for the aforementioned applications in their study. Their results stated that the collector's average yearly efficiency was about 60%, while the ORC electric system's average yearly efficiency was roughly 6%. Luis Cortes et al. [56] developed multigeneration systems for building systems. They introduced techniques to decrease water usage by as much as 75% and emissions by 74%. Hands and his group [57] assessed the benefits in energy and efficiency of a trigeneration system. They have used ST collectors to generate hot water for their intended system. According to the data, the utilization of this collector for the purpose of water heating resulted in a 21% reduction in the annual energy consumption. They have reported that, solar energy was responsible for providing up to fifty percent of the energy required for the heating of space, while the solar-driven desiccant cooling system was responsible for thirty-five percent of the overall space cooling. A numerical model was constructed by Soutullo [58] in order to evaluate the energy performance of a polygeneration plant under a variety of different scenarios. The thermal model in this simulation was developed with a combination of St collectors and biomass boilers. Furthermore, solar panels and wind turbines were operated autonomously alongside fuel cells. Their results indicated that optimal performance might be attained through system combinations.

2.4 PVTST literature review

In this part of the literature review, numerical and experimental PVTST system studies are introduced and reported. A few researchers have focused on the PVTST systems; for this reason, it seems that this field needs to be covered more. In this context, a two-dimensional PVTST system was introduced by Ma [59]. This work investigates the effects of using PVT systems, both with and without glass, independently and connected in series with the ST system. PVTST had superior thermal efficiency and energy conservation compared to the other collectors, according to their findings.

Li et al. [60] investigated four cases of glazed and unglazed PVTS systems. According to their results, among the several collectors, the PVTST with glazing shown the highest performance in term of energy and exergy efficiency. While the exergy efficiency was observed at 17.63%, the energy efficiency was recorded as 41.51%. Within the scope of their research, Kazemian and his team [61] employed the Taguchi technique to carry out a numerical analysis with the purpose of optimizing the PVTST system. Their optimization increased the heating capability of the entire system by 35.78% and electrical energy efficiency by 23.86%, respectively. Z. Han and colleagues [62] conducted an evaluative study on the thermal and electrical behavior of the PVTST systems. As per their investigation, the PVTST system may generate hot water with a higher temperature than the PVST system. According to them, in high-radiation circumstances the PVTST system provides better advantages. These benefits will, however, progressively drop as the inlet water's temperature goes up. Chandan and his group carried out the first experimental and numerical study on PVTST [63]. The experimental investigation examined glazed and unglazed PVT systems arranged in series with the ST system. The study included energetic and exergetic efficiencies. The glazed one showed a maximum temperature of 67 °C, whereas the other one had 63 °C. According to their analysis, the unglazed PVTST system's thermal efficiency increased by 55–60%. The effect of adding nanofluid or PCM into PVTST systems on their thermal behavior has been studied several times. Kazemian and his team [64] employed various combinations of nanofluids while working with a PVTST system and conducted an analytical comparison of the outcomes. Comparatively to other nanofluids, the computational investigation found that the multiwall carbon-silicon carbide nanofluid had the highest thermal productivity at 56.55%.

Using a variety of PCM and a range of fluid flow rates, Alikhan [65] conducted an investigation of the PVTST system effectiveness. The results indicated that across all fluid flow rates, the incorporation of PCM elevated the outlet temperature of the system while reducing the surface temperature of the PV, thus enhancing energy production and exergy efficacy.

2.5 literature review of the PVT and ST systems applications

highlighting the employing of hot water output from the PVTST system as a possible energy source, this part of the thesis explores the literature on the applications of PVT and ST systems in residential purposes. The production of hot water by ST or PVT collectors is vital, since it assists in alleviating the growing need for fossil fuels. Consequently, professionals in this field have carried significant computational and empirical investigations to assess and lower the energy consumption for household hot water or heating space.

A computational model utilizing PVT systems was undertaken by Hamdoon et al. [66]. Six PVT collectors have been utilized to supply hot water for a family of five persons. The surface area of each was 1.5 m^2. The system has been reported to deliver hot water at a range of 61.7% to 83% efficiency. Liang and his colleagues [67] performed a computational investigation to explore the viability of using 32 m^2 of the

PVT systems for heating a certain volume. The study indicates that, in the absence of the supplementary heater, the system effectively managed the required load from midnight to 6 p.m. Glembin [68] employed several thermal distribution systems. An indirect, a combi, and a direct solar collector with heating components were included in this category. According to their results, by utilizing the combisystem, they were able to achieve significant reductions in energy consumed.

Herrando and his team [69] investigated hot water and electricity generation utilizing PVT systems. They developed a mathematical model for nine forms of PVT systems, each with a surface area of 1.62 m^2 per collector. According to the findings that they obtained, this system is capable of satisfying 36% of the requirements for hot water. Lu, together with his colleagues [70], proposed a space heating system by using a solar seasonal storage as a thermal energy supplier.

The findings of their research revealed that a system with a 40 m^2 solar collector and a 40 m^3 reservoir might fulfill the energy requirements for heating a 240 m^2 area. Several studies within the same domain may be found in [71]. References [72] and [73] provide more insights, while numerous real projects can be located in [74].

Chapter 3
Operational Methods

3.1 Overview

This part covers a comprehensive description of the experimental facilities of the current thesis. This description encompasses the specific materials and apparatus that were employed, as well as the procedures that were implemented to collect and assess the necessary data for completing the main target of the experiment. Furthermore, this section offers a model and simulation of the experimental work, as well as a comparison of the results.

3.2 Physical setup

The testing facilities of the present study was established in Hindia, Babil, Iraq, corresponding to the coordinates 32.32◦ North and 44.10◦East. A pair of PV solar panels are coupled with a heat exchanger to harness the additional heat produced on their surfaces. The total power capacity of each panel is 160 W, and it encompasses a surface area of 1 m^2. The heat exchanger is made up of one sheet and eight tubes, all of which are placed in a systematic manner and are mounted to the back of each pv panel. In addition, glass wool insulator is utilized to insulate the uncovered side of the heat exchanger so as to enhance the thermal insulation. For the purpose of ensuring that the tubes are attached to the absorber plate in the appropriate manner, mechanical tools are utilized. The PVT system is sequentially connected to 2 m^2 of the ST collector, represented by the flat plate collector as previously mentioned. In this way, the warm water exits the PVT collector and enters the ST collector directly. The ST collector includes the essential elements observed in a PVT collector, which involve a glass cover, an absorber plate, eight pipes spaced 10 cm apart, and an insulator. Both Table 3.1 and Table 3.2 provide comprehensive information regarding the physical description and general specifications of the materials utilized in the PVT and ST systems.

During the experiment, data was collected using TK7Y data acquisition device. Temperature measurements were conducted utilizing PT 100 sensors, with an accuracy of ±1% over a broad spectrum of -30°C to 500°C. In order to monitor and adjust the flow of water, a K-100 flow meter was utilized. This meter ranged from 0.2 to 2 Liters per minute, and it had an accuracy of precisely ±2.5%. Figures 3.1 and 3.2 represent schematic representation of the experimental procedure alongside the real arrangement.

3.3 Operating conditions

Both collectors, PVT and ST were oriented southward at an angle of 35° and 45°, correspondingly. To cover a broad spectrum of weather over the test area, the test days were scheduled for first of January, February, March, and April. Every day of the experiment was absolutely clear. During each day of the test, the average wind speed was measured. The collection of data was scheduled to take place between the intervals of 10 a.m. to 4 p.m. The database of the website www.tutiempo.net was utilized in order to collect information regarding wind speed and the solar radiation.

Table 3.1: PVT materials properties

materials	description	thermal conductivity W/m.k	density kg/m3	specific heat capacity J/kg.k
PV	poly-crystalline (160 w)	148	2330	700
Absorber Plate	copper (1.48X0.68X0.0007) m	400	8940	385
Pipes (8)	copper(D=0.001, L=1.4) m	400	8940	385
Insulation	glass wool(1.48X0.7X0.3) m	100	0.035	1800

Table 3.2: ST materials properties

materials	description	thermal conductivity W/m.k	density kg/m3	specific heat capacity J/kg.k
Glass	low-iron glass (2X1X0.0035) m	1	2450	500
Absorber plate	copper (1.95X0.95X0.0004)m	400	8940	385
Pipes (8)	copper (D=0.001, L=1.88)m	400	8940	385
Insulation	glass wool (2X1X0.03) m	100	0.035	1800

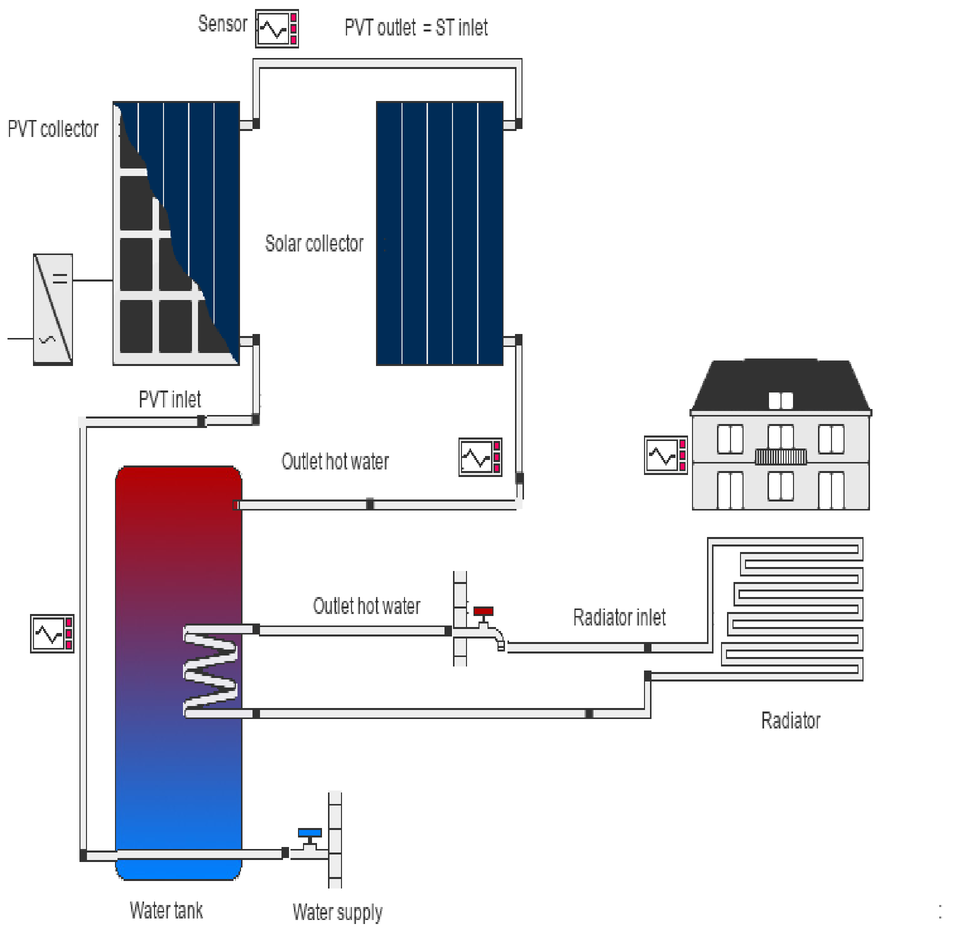

Figure 3.1: Experimental work schematic

3.4 Numerical solution

Simulations can facilitate a more profound understanding of the investigation and support the experimental work methodology. The computer fluid dynamic principles (CFD) were employed to conduct the current simulation. CFD is a computer simulation of fluid flow to forecast the behavior of fluids under different conditions. It solves the governing equations of fluid dynamics using an algorithm and numerical approach, thereby obtaining comprehensive knowledge about the flow field [75]. Generally, CFD procedures consist of geometry designing, meshing generation, boundary conditions, system equation solving, postprocessing, or results visualization. The SolidWorks program was used to develop the geometrical structure of the PVT and ST collector systems.

Figure 3.2: Actual experimental work

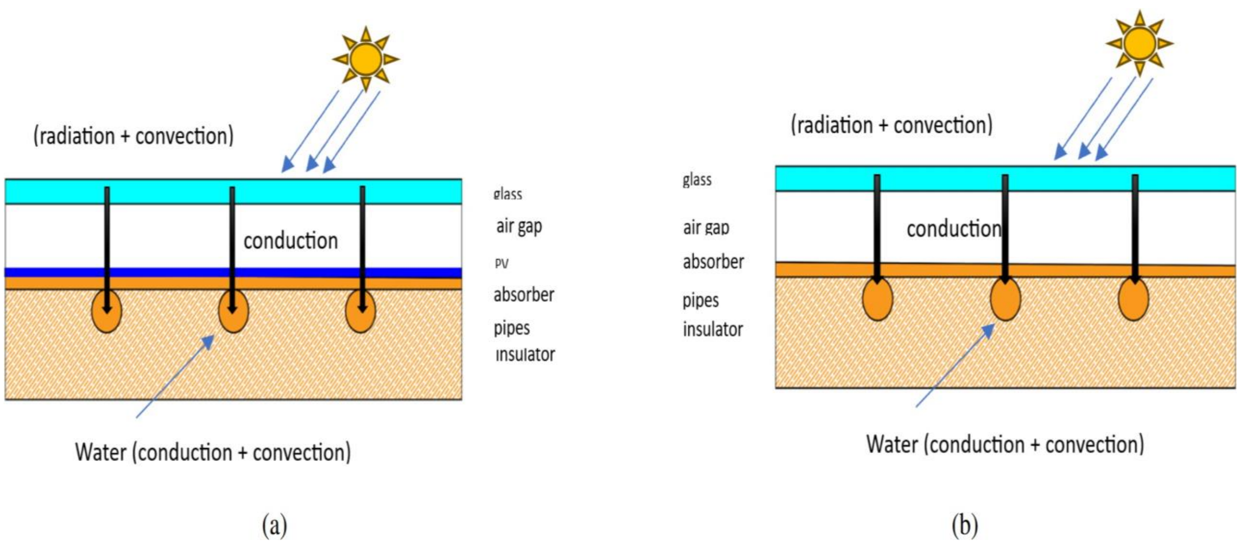

Figure 3.3: General design of the geometry for: a. PVT system, b. ST system

It is recommended that any design approach be prepared in a manner that minimizes the overall number of grid elements to simplify the problems and reduce their solution time. In this context, the computational domain was limited by the utilization of a numerical 3-D model that featured a single pipe or riser from each collector. Regarding the layers of the geometry employed, it was presumed that the back sheet and tedlar were combined with the PV cells and viewed as a single layer [76]. The construction of the overall PVT and ST systems modelling is depicted in a detailed way in Figure 3.3. Ansys 21 package, a sophisticated software that was developed to deal with engineering problems via the integration of computational fluid dynamics (CFD) methodology, was used to carry out each and every computer simulation of the PVT and ST systems in an independent manner. When dealing with problems involving fluid dynamics, it is vital to determine whether the flow is laminar or turbulent in order to select the appropriate model and the method for solving the problem. By calculating the Reynolds number (Re), which is an illustration of the relationship between the viscous and inertia forces, it is possible to demonstrate the flow behaviour. The flow is considered to be laminar when Re is less than 2300, and it is considered to be turbulent when it is larger than 4000 [77]. Given that the Re value in the current work was below 2300, the flow was considered laminar. Each system's presuppositions and boundary conditions are defined as the following ways:

- $V = V_f$ is what the pipe inlet velocity is when using a constant fluid velocity of 0.106 m/s.
- In relation to the fluid inlet temperature, $T = T_i$, under variable temperature conditions, as it varies depending on the temperature of the source's tank in each instance.
- Both incompressible and steady state conditions were considered for the fluid flow within the pipes.
- A condition of no slip or zero wall velocity was assumed.
- A pressure outlet condition was implemented for the pipe outlet: $P=P_o$.
- Every interval of the current study, the top layer of the glass was subjected to a consistent heat flow flux and free convection, depending on the outside temperature and irradiation levels.
- Solid layers heat generation is neglected.

Heat transmission mechanisms encompass conduction among the solid layers (glass, photovoltaic cells, absorber plate, pipe) and convection between the internal pipe surface and the fluid that flows [78]. It is worth noting that through modeling, the ST and PVT systems have the same boundaries; hence, the difference between them is just in PV cells and their layers (tedlar and back sheet), which were considered as one layer, as mentioned recently. Both the absorber plate's outside and the pipe's bottom half are heat-insulated.

3.4.1 Equations and Computational Techniques

The characteristics of the flow of fluid are described by the governing equations of momentum, energy, and continuity, which are defined in the following [76]:

$$\frac{\partial(\rho u_j)}{\partial x_j} = 0 \tag{3.1}$$

$$\frac{(\partial \rho u_i u_j)}{\partial x_j} = -\frac{\partial P}{\partial x_i} + \frac{\partial}{\partial x_j}\mu\left[\left(\frac{\partial u_i}{\partial x_j} + \frac{\partial u_j}{\partial x_i}\right)\right] \tag{3.2}$$

$$\frac{(\partial \rho u_i u_j)}{\partial x_j} = \frac{\partial}{\partial x_j}k\left[\left(\frac{\partial T}{\partial x_j}\right)\right] \tag{3.3}$$

The solid domain equation can be stated as follows: [63]:

$$k_s \nabla^2 (T_{\text{solid}}) = 0 \tag{3.4}$$

where K_s: represents the thermal transfer property, T_s : is the solid temperature. The equations that describe convective heat transfer as well as the radiation can be expressed as follows [63]:

$$Q_c = h_c A(T_a - T_g) \tag{3.5}$$

$$Q_{rad} = \varepsilon A \sigma (T_g^4 - T_{sky}^4) \tag{3.6}$$

where: T_a refer to the ambient temperature, T_g is the glass temperature, and T_{sky} is the sky temperature, σ : denote to the Stefan Boltzman constant; and ϵ : represent the emissivity. The convective heat transfer coefficient h_c can be stated by the following equation [63]:

$$h_c = 3.8 + 5.7v \tag{3.7}$$

where v : represent the speed of the wind, The following equation express the sky temperature [63]:

$$T_{sky} = 0.0552 * T_a^{1.5} \tag{3.8}$$

It is possible to express the energy or thermal efficiency in the following way [79]:

$$\eta = \frac{Q_{th}}{GA} = \frac{m \cdot C_p (T_o - T_i)}{GA} \tag{3.9}$$

$m.$: describe the fluid flow rate, C_p : denote to the heat capacity, G : represent the solar irradiance, T_i and T_o : are denote to the inlet and outlet water temperatures, respectively.

The electrical efficiency of the PV solar panel can be expressed as the following equation [80]:

$$\eta_{el} = \eta_{ref} - \mu(T_{pv} - T_{ref}) \tag{3.10}$$

In the given equation, η_{ref} : represents the baseline or standard efficiency with respect to the standard conditions ($\text{G} = 1000\text{w/m}^2, T_{PV} = 25\ ^\circ\text{C}$). Additionally, T_{ref} : represents the reference temperature, while μ represents efficiency temperature coefficient. The term "exergy efficiency" refers to the ratio of the system's useable exergy, also known as thermal exergy, to the exergy generated by solar radiation. This ratio can be expressed as [81]:

$$\xi = \frac{mC_p\left[T_o - T_i - T_a \ln\left(\frac{T_o}{T_i}\right)\right]}{GA\left[1 - \frac{T_a}{T_s}\right]} \tag{3.11}$$

where T_s, represents the sun temperature and it's approximately to 75% of the perfect black surface temperature. The value of this parameter, which is an essential component for solar radiation exergy, can be approximated to be 4350 K [82][83]. The model solver commences by initializing the input values for the following parameters: inlet and ambient temperatures, solar radiation intensities, wind speed, and electrical efficiency. After that, it solves the governing equations using the boundary conditions in order to determine the temperature of the solar cell as well as the solar cell temperature. Utilizing the second-order upwind method, the solver discretized the equations involving momentum, energy, and pressure. The residual is a metric that quantifies the degree of similarity between the numerical solution and the actual physics model. Figure 3.4 depicts the flowchart illustrating the procedures for determining the outlet water temperature.

The residuals of the utilized equations were 10^{-6} for momentum and mass equations and 10^{-4} for the continuity equation.

3.4.2 Grid independent

A standard verification method for CFD entails making multiple adjustments to the number of mesh elements and evaluating the effect of these changes on the solution. To attain solution verification, it is advisable and commonly accepted to finalize the solution with particular grid elements and thereafter raise them multiple times while checking out the results. If results remain unchanged with grid modifications, then the grid is deemed enough for the solution processes. Conversely, if the solution varies, it indicates that the grid requires refinement until solution stability is achieved. Re-meshing is necessary for achieving solution stability. In order to generate the necessary mesh, the present investigation implemented Ansys Fluent Meshing software. Mesh refinement was performed on the interfaces that are in contact or immediately subjected to solar radiation. As a result of the current mesh operations, the final and dependent meshes have orthogonality assessed at 0.2, indicating high mesh quality. The mesh procedure involved creating many meshes until stability was attained at three distinct grids, where the solutions began to exhibit steadiness and remained unchanged with a growth of the mesh elements. In other words, the water outlet temperature of both collector systems ST and PVT was computed until the answer was independent of the grid. The grid cells that were utilized for the ST and PVT systems, were composed of 1,015,108 and 750,000, respectively. A sectional front view of the used mesh is shown

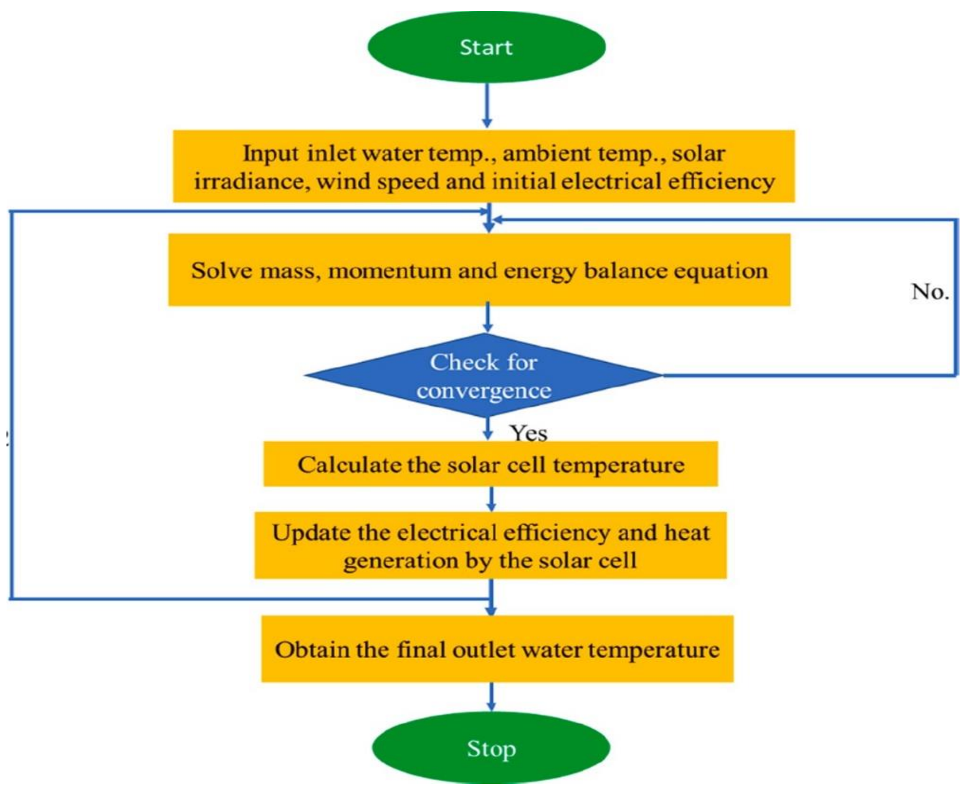

Figure 3.4: Numerical solution flow chart

in Figure 3.5, which also includes solution verification for the both PVT and ST systems. For the purpose of ensuring that the outcomes of the computer simulation are accurate and valid, they were compared to experimental data that was collected throughout this specific study. For the particular day of January , the outlet temperature data that was acquired from the computer simulations for the both PVTST and ST systems, were computed, and then compared with the experimental values. The results of the current investigation shown a good match between experimental and simulation results as illustrated in Figure 3.6, where the maximum error was 6.74 %.

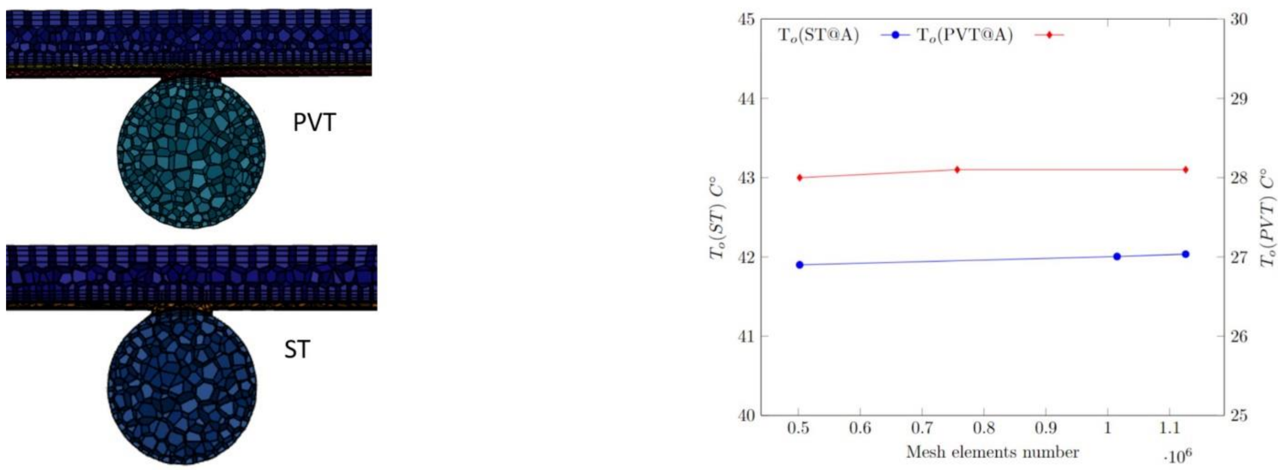

(a) (b)

Figure 3.5: a. Mesh geometry of PVT and ST systems, b. Mesh independent verification

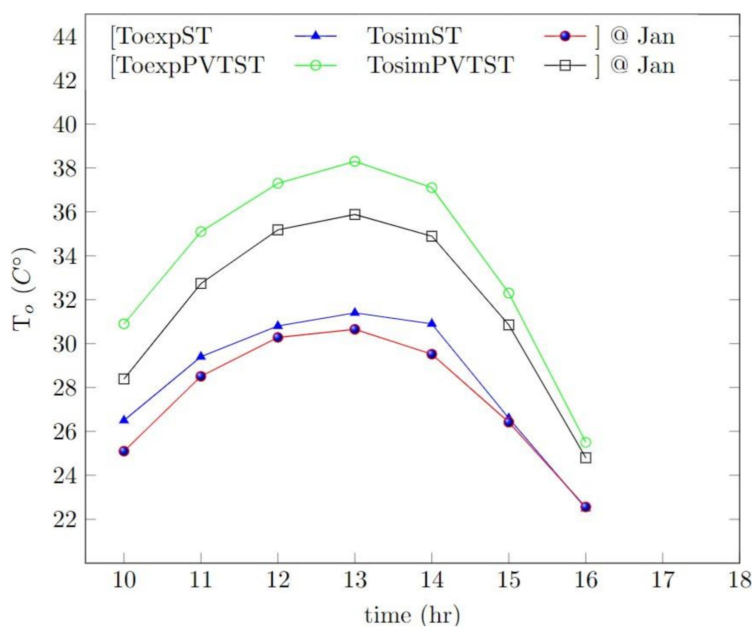

Figure 3.6: Numerical results validation

Chapter 4
Results

Following what has been reported in the literature, the present work uses both experimental and numerical approaches to assess the thermal performance of the combined or hybrid system throughout several days in different months during the prescribed year. In this context, the fundamental performance indicators that are being considered during this study are exergetic and energetic efficiency. In addition, this investigation encompasses the simulation of heating a single room by employing the PVTST or ST systems as a hot water provider, along with the determination of the temperature deficiency of the hot water demand by concurrently employing the same systems.

4.1 Solar radiation

There are two forms of solar radiation that can reach any particular location on the earth: direct radiation and diffuse radiation. These two types of radiation are added together to form what is also referred to as global solar radiation [84]. The term "global solar radiation" refers to the entire amount of solar radiation that is received by the surface of the Earth and serves as the primary source of energy for all forms of life that exist on Earth [85]. A representation of the solar radiation amounts from 10 a.m. to 4 p.m. for experimental days is depicted in Figure 4.1. Additionally, the second segment of this graph depicts the monthly global radiation levels for the years 2022 and 2023. The data regarding monthly global radiation and average temperature for the specified location over the indicated years is thoughtfully collected in Table 4.1 [86]. Given the observations in this table, the magnitudes of solar radiation can be considered to be at acceptable levels in the study's location, which is characterized by favorable solar conditions. There is a potential for effective solar energy generation, particularly during the summer months when radiation is at its maximum, as indicated by the global radiation values. For the years given, the temperature data indicates that the temperature ranged from 11.9°C in January to 39.6°C in August. These temperatures are common in multiple fields, especially the solar energy field, and besides that, they may have a detrimental impact on PV systems. For the given particular days respectively, the solar radiation's total energy was (3513, 4234, 4467, and 5000) $W/m^2/day$.

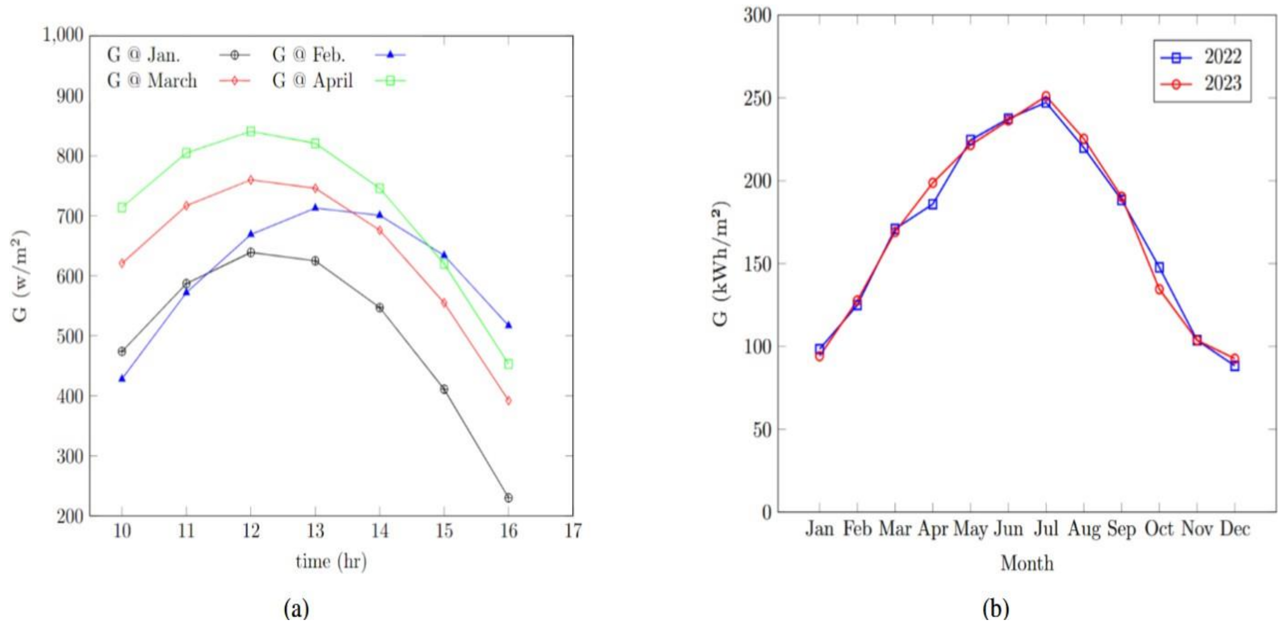

Figure 4.1: Solar radiation for: a. (10 am-4 pm.) of the experimental days, b. monthly average magnitudes of the years 2022 and 2033

Table 4.1: monthly global horizontal irradiation (G) and average temperature data

Month	2022 G (kWh/m2)	2023 G (kWh/m2)	2022 Temp (°C)	2023Temp (°C)
January	98.35	94.12	11.9	12.0
February	124.98	127.74	16.5	13.8
March	170.89	169.07	18.0	19.5
April	185.86	198.72	26.9	24.6
May	224.54	221.57	30.5	30.9
June	237.45	236.38	37.3	35.9
July	247.19	250.99	38.1	38.8
August	219.88	225.30	39.1	39.6
September	188.39	190.35	35.2	35.5
October	147.72	134.56	30.1	28.8
November	103.80	103.73	20.4	20.1
December	88.28	92.60	14.9	15.5

4.2 Fluid outlet temperature

The solar collector output temperature is an essential factor influencing its thermal efficiency, hence affecting its appropriateness for various thermal applications. Solar collector system design, solar irradiance, initial fluid temperature, and flow rate all have an impact onits output temperature.The factors' effects could be precisely described as follows:

1. Solar radiation: under constant fluid flow rate and inlet temperature, the peak outlet temperature is reached when solar radiation incident on the solar collector is at its highest level.

2. Flow rate: The flow rate of the used fluid can influence the quantity of heat that can be absorbed and then transmitted. Increasing mass flow rates often result in decreased outlet temperatures owing to enhanced heat capacity and accelerated fluid motion, which shortens the duration for heat absorption.

3. Inlet temperature: Outlet temperature depends on the fluid inlet temperature. The maximum possible outlet temperature can be considerably raised by raising the input temperature.

4. The design of the solar collectors profoundly influences their outlet temperature, which is essential for optimal thermal energy applications. Elements, such as collector type, surface area, flow configuration, and material qualities. They are absolutely important in determining how well a solar collector transforms solar energy into thermal energy. According to the current experimental configuration, the PVT output water temperature serves as inlet water temperature of the ST collector. The source water initially enters the PVT collector, acquiring thermal energy that elevates its temperature by several degrees before being delivered to the ST collector and gaining a new heating energy magnitude. The aforementioned approach enhances the heating efficiency of the entire system and raises the outlet temperature. Figure 4.2 illustrates the inlet, outlet, and ambient temperatures of the PVT, ST, and PVTST systems. This figure illustrates that the thermal energy introduced via the PVT collector and subsequently transferred to the ST collector as an inlet water temperature leads to in the highest output temperature for the PVTST system when compared to the standalone ST system. Throughout the duration of the four testing days, the outlet temperature of the PVTST system exhibited an increase of (6.15, 6.65, 7.51, and 5.48) °C when compared to the ST collector.

4.3 Energy efficiency

The energy output of the system was thoroughly collected and analyzed in accordance with the designated experimental days. For the purpose of projecting the total output energy of the PVTST system, the output energy of each collector was estimated independently. Compared to the ST collector, the output energy of the PVTST system raised by a mean values of (213.71, 231.07, 265.78, and 190.41) W throughout the course of the four days, as indicated by the findings. Table 4.2 illustrates the output energy results for all collectors during the test. This table provides a comprehensive analysis of the energy output from three types of solar energy collector systems: PVT, ST, and a combined system (PVTST), over the initial four months of the year. The data is presented in terms of global solar irradiance and energy outputs. In January, the global solar irradiance fluctuated between 230 and 629 W/m2. The PVT system produced energy outputs ranging from (116.28 to 272.47) W, while the ST system delivered outputs between (190.9 and 513.71) W. The combined PVTST system consistently outperformed the individual systems, with energy outputs spanning from (295.04 to 739.33) W.

February saw an increase in solar irradiance, with values ranging from (428 to 713) W/m2. The PVT system achieved energy outputs between (253.38 and 339.32) W, while the ST system ranged from (329.75 to 558.84) W. The PVTST system demonstrated its superior efficiency, delivering outputs between (572.72 and 857.35) W. In March, irradiance values rose further, ranging from (392 to 760) W/m2. The PVT system produced energy outputs between (166.61 and 295.04) W, while the ST system ranged from (312.39 to 586.6) W. The PVTST system maintained its dominance, with energy outputs spanning from (465.12 to a peak of 839.99) W. April exhibited the highest levels of solar irradiance, ranging from (714 to 841) W. The PVT system's energy output varied between (111.07 and 277.68) W, while the ST system ranged from (354.04 to a maximum of 638.67) W. Once again, the PVTST system delivered the highest performance, with energy outputs between (458.17 and an outstanding maximum of 895.83) W. In summary, it can be said that the energy output across all systems increased with higher solar irradiance, peaking in March and April and the combined PVTST system consistently outperformed both PVT and ST systems individually, showcasing its ability to harness solar energy more effectively.

While all systems exhibited variability based on irradiance levels, the PVTST system demonstrated robust performance across all months. A solar collector’s thermal efficiency measures how much energy is converted within the collector. It is presented as the effective heat generation to accessible irradiation ratio. Consequently, improving thermal efficiency means increasing the amount of the collector useable energy generated.

It was assessed beneath a variety of operational conditions throughout the duration of the study. The ST and PVTST systems' thermal efficiencies are illustrated in Figure 4.3. There is an expectation that the thermal efficiency of the PVTST system becomes greater than that of the ST collector. This follows from a significant change in the temperature difference part in equation 7, which raises both thermal efficiency and usable energy.

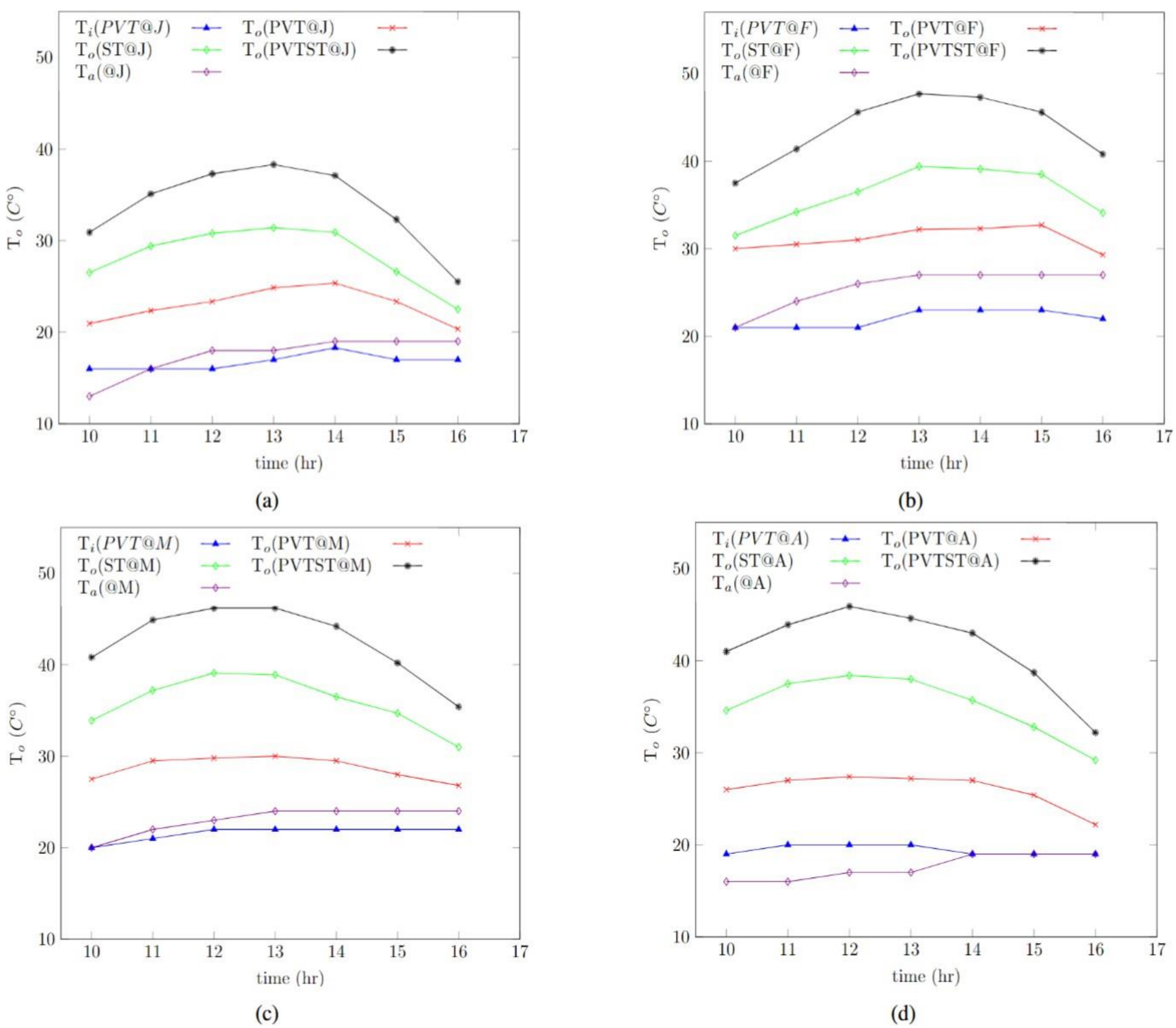

Figure 4.2: Inlet, outlet, and ambient temperatures of the PVT, ST, and PVTST systems

When compared to the ST collector, the PVTST system demonstrated an average boost in the thermal efficiency estimated by (24.8, 18.2, 22.3, and 19.4) %, respectively, throughout each of the selected four days.

The PVTST system's thermal efficiency demonstrates substantial and obvious variations over the course of the specified days, primarily as a result of its elevated potential energy in comparison to the ST collector. Figures 4.4 and 4.5illustrate the thermal efficiency behavior relative to the inlet-ambient temperature difference (Ti − Ta)/(G) for the both collectors used, ST and PVTST within the study periods. According to the data, it is possible to improve thermal efficiency and, as a result, reduce heat losses by lowering the temperature gap between the input and the ambient temperature. Additionally, attention to fluctuations in radiation levels is crucial, as these may exacerbate heat losses and diminish thermal efficiency.

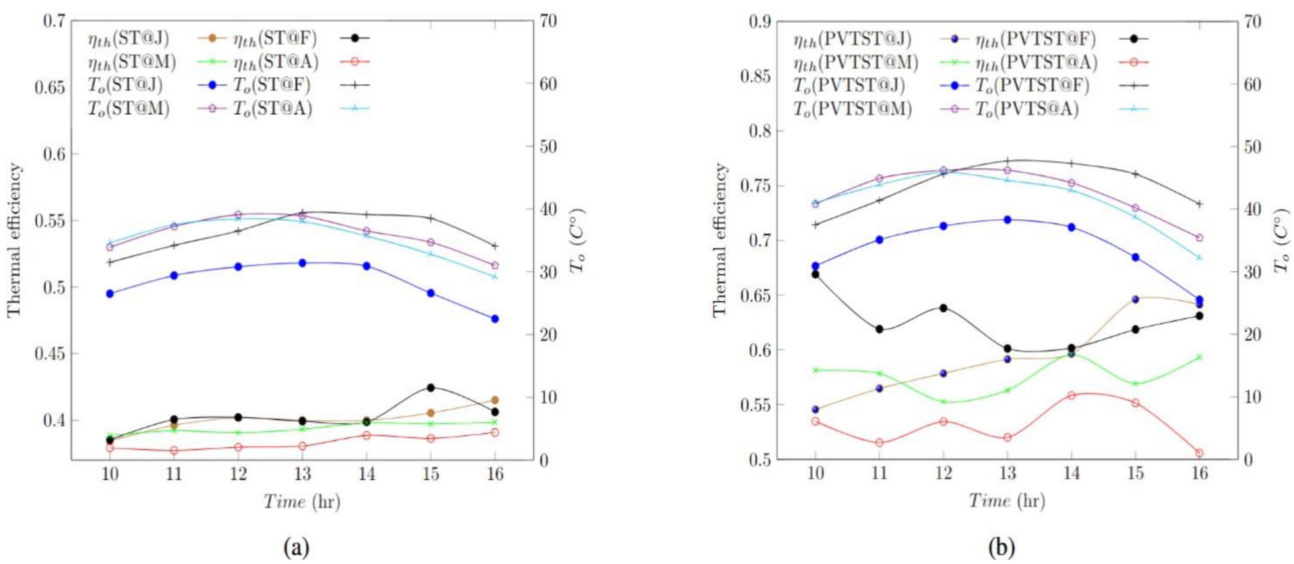

Figure 4.3: ST and PVTST thermal efficiency

4.4 Exergy efficiency

A system's exergy efficiency is a metric that quantifies the degree to which it converts the accessible energy or energy on hand into beneficial work. Beyond the context of the energy efficiency, it offers a comprehensive insight of how the entire system works. Within the scope of this study, the exergy efficiency of both ST and PVTST systems were assessed during the length of the investigation. As the results of the tests demonstrate, the exergy efficiency of the PVTST system rose

Table 4.2: Harvested collectors' energy(W)

	G W/m²	PVT energy	ST energy	PVTST energy		G W/m²	PVT energy	ST energy	PVTST energy
January					March				
	474	171.47	364.46	517.18		621	260.32	482.47	721.98
	587	220.41	465.12	662.97		717	295.04	562.31	829.58
	639	255.12	513.71	739.33		760	270.74	593.55	839.99
	625	272.47	499.83	739.33		746	277.68	586.6	839.99
	547	244.7	437.35	652.55		676	284.62	503.3	770.57
	411	220.41	333.22	531.07		555	208.26	440.82	631.73
	230	116.28	190.9	295.04		392	166.61	312.39	465.12
February					April				
	428	281.15	329.75	572.72		714	242.97	541.48	763.63
	572	277.68	458.17	708.09		805	242.97	607.43	829.58
	669	347.1	538.01	853.88		841	256.85	638.67	899.00
	713	319.33	569.25	857.35		821	249.91	624.79	853.88
	701	322.8	558.84	843.46		746	277.68	579.66	833.05
	634	336.69	538.01	784.45		620	222.14	479.00	683.79
	517	253.38	419.99	652.55		453	111.07	354.04	458.17

by an average of (7.98, 7.45, 7.82, and 6.97) % in comparison to the ST collector throughout the course of the four test days, respectively. Boosting the energy efficiency directly relates to the general quality of the system since it means increasing the quantity of the produced useable energy. Equation 9 demonstrates that multiple parameters, mainly solar radiation, inlet & outlet fluid temperatures, and ambient temperature, affect the exergy equation. As such, knowing the particular exergy approach is challenging since it varies depending on the environment and operational settings. The current investigation demonstrates, as depicted in Figure 4.6, that an increase in the temperature of the surrounding environment typically results in a decrease in the exergy efficiency in all of the scenarios that were evaluated.

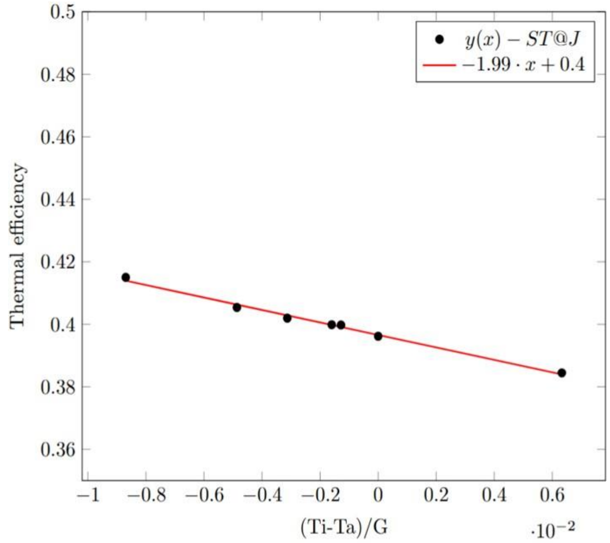

(a)

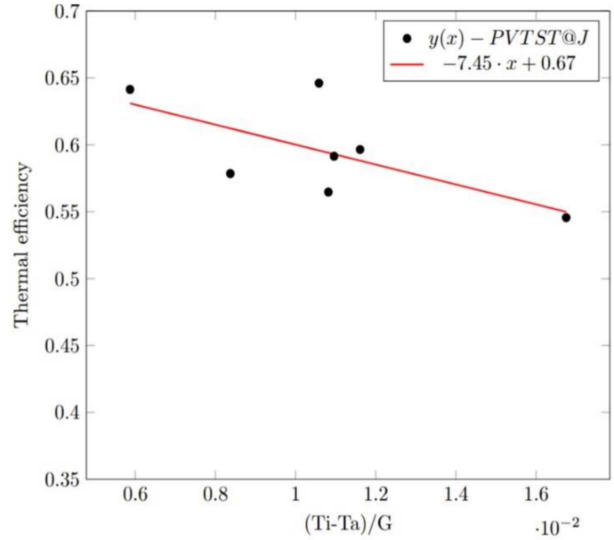

(b)

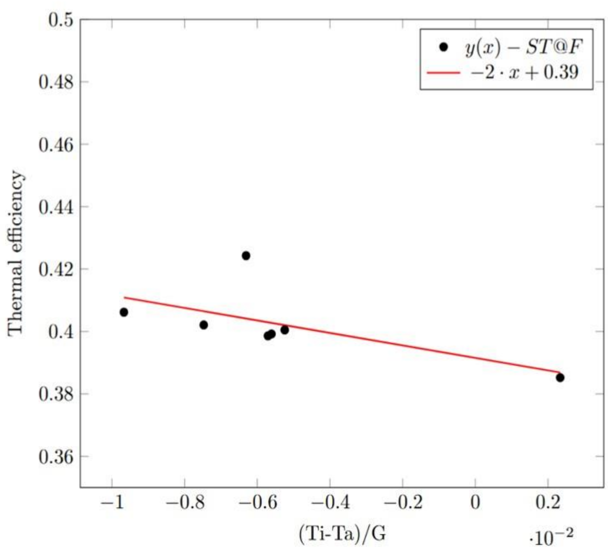

(c)

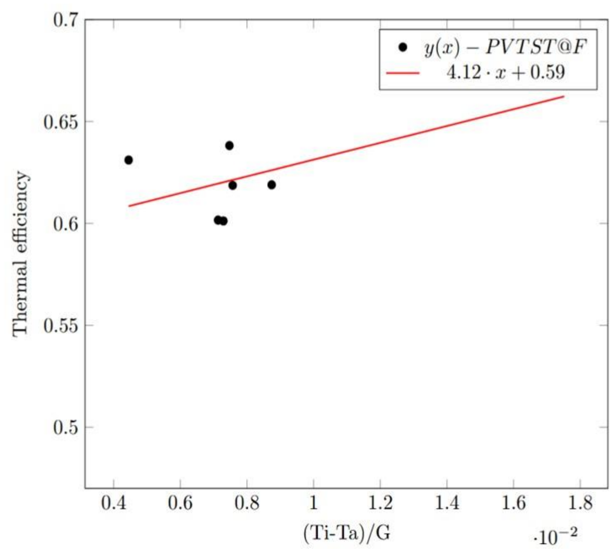

(d)

Figure 4.4: Thermal efficiency behaviour relative to the inlet-ambient temperature difference for January and February

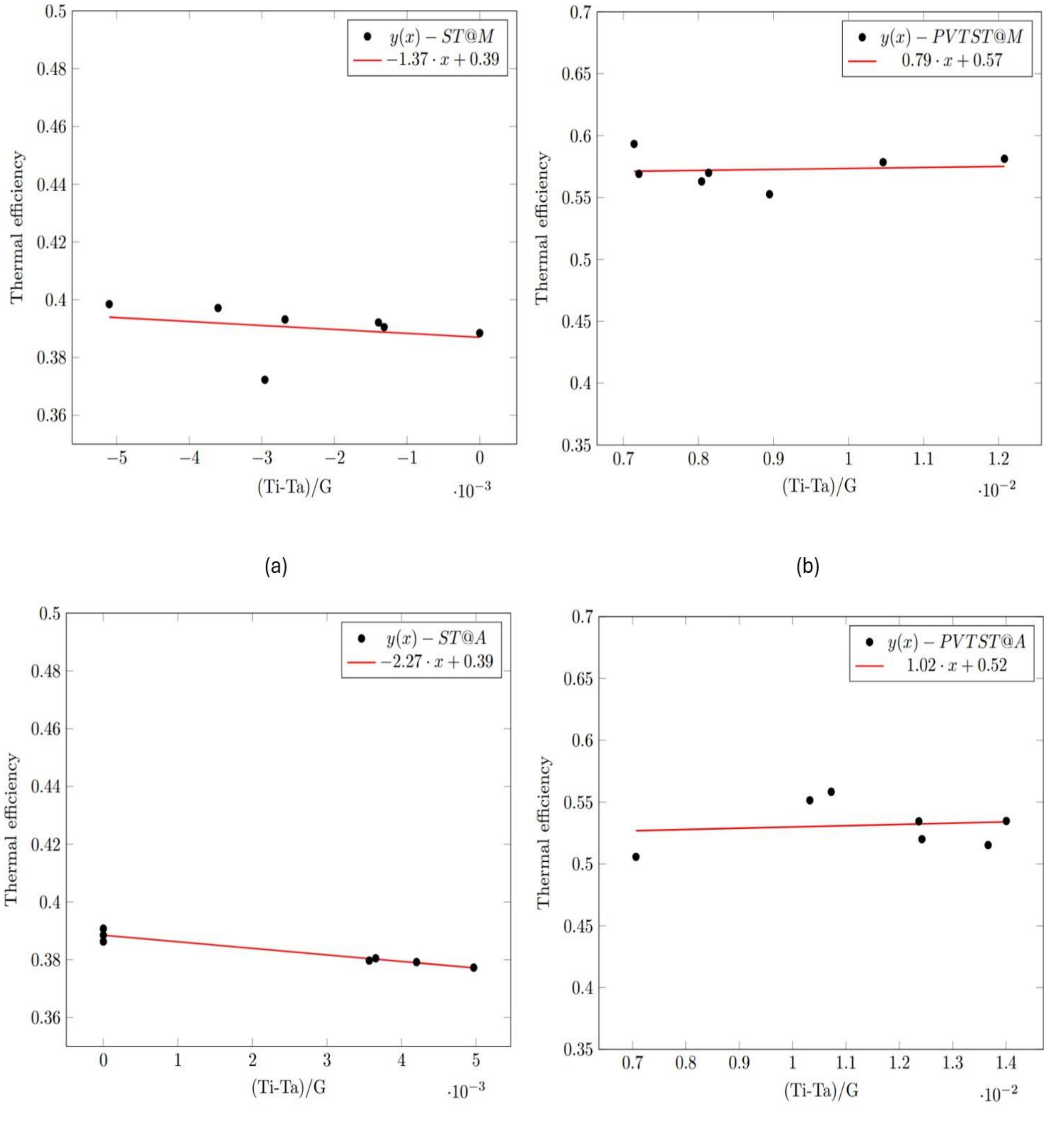

Figure 4.5: Thermal efficiency behavior relative to the inlet-ambient temperature difference for March and April

4.5 Electrical efficiency

The capacity of a solar panel to convert solar radiation into electrical power that can be utilized is referred to as its photovoltaic (PV) electrical efficiency. This efficiency depends on various factors, including the type of photovoltaic material, operating temperature, irradiance levels, and system losses. Typically, monocrystalline panels achieve efficiencies between 18–22%, polycrystalline panels range from 15–18%, while thin-film technologies have lower values around 10–14%. External influences such as dust accumulation, shading, and aging of the panels also affect performance. According to the research studies, increasing the temperature of the PV panels results in a decrease in both their electrical efficiency and their energy output. As temperature rises, efficiency tends to decrease due to the negative temperature coefficient of PV cells. In another word, PV panels are generally produced with a temperature coefficient, indicating the rate of decline in their electrical efficiency for each one-degree rise in temperature. A one-degree rise over the average standard temperature decreases electrical efficiency by 0.35%/°C, according to the panel's temperature coefficient. Higher-efficiency modules are advantageous in space-constrained applications, though they may come with higher costs [87].

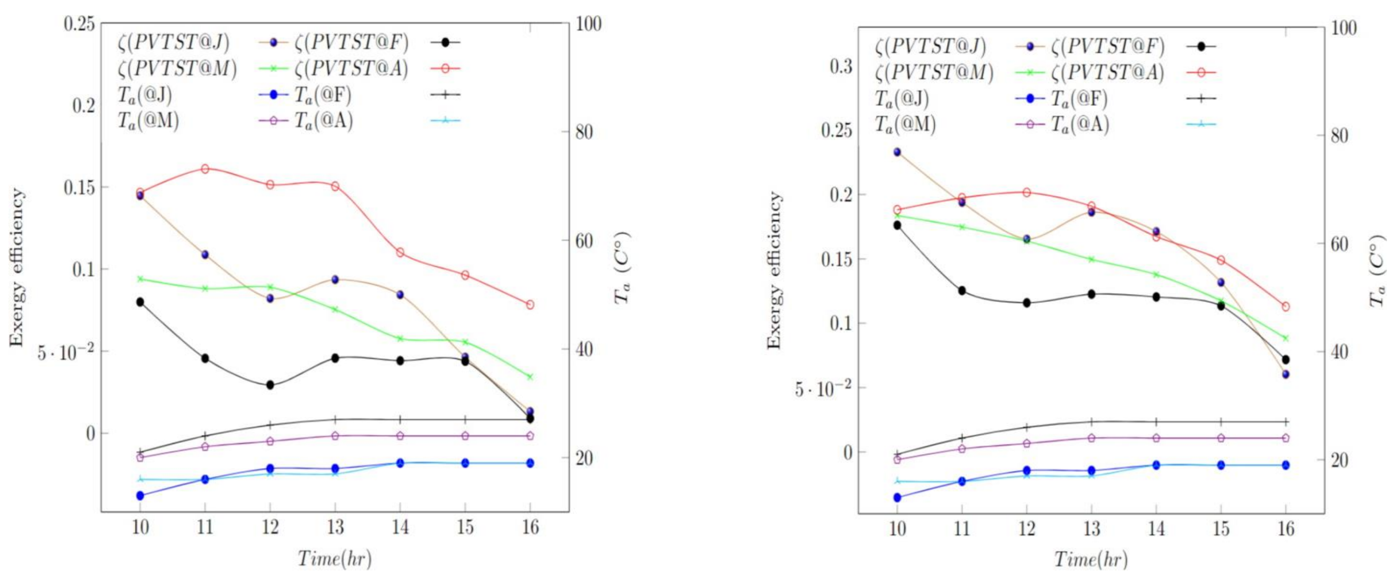

(a) (b)

Figure 4.6: Exergy efficiency during the experimental days for: a. PVTST system, b. ST system

In this context, maintaining the temperature of the PV panel as near to the norm as practically possible can help to reduce energy losses.

Both collectors' electrical efficiency through the study period can be shown in figure 4.7. The PVT system achieves a decrease in the average temperature ranging from 6 to

11 °C. In comparison to traditional PV panels, this reduction enhances electrical efficiency, yielding average improvements of (31.04, 41.16, 47.34, and 11.55) % within the four experimental days, respectively.

4.6 Heating system for individual rooms

solar energy presents a sustainable and eco-friendly alternative to conventional fossil-fuel-based systems. By capturing and utilizing the sun's thermal energy, solar space heating systems can significantly reduce fuel consumption, lower greenhouse gas emissions, and contribute to energy independence. The concept involves collecting solar radiation through solar thermal collectors, which transfer the absorbed heat to a working fluid—typically air or water. This heat can then be distributed through radiators, underfloor systems, or air ducts to maintain indoor comfort levels. Solar heating systems may operate independently or be integrated with auxiliary heating units to ensure continuous operation during periods of low solar availability. There are several types of solar space heating systems, such as passive solar heating, which relies on building orientation and materials to store and distribute heat naturally, and active systems, which employ pumps, fans, and controls to manage heat transfer more efficiently. Given the growing interest in

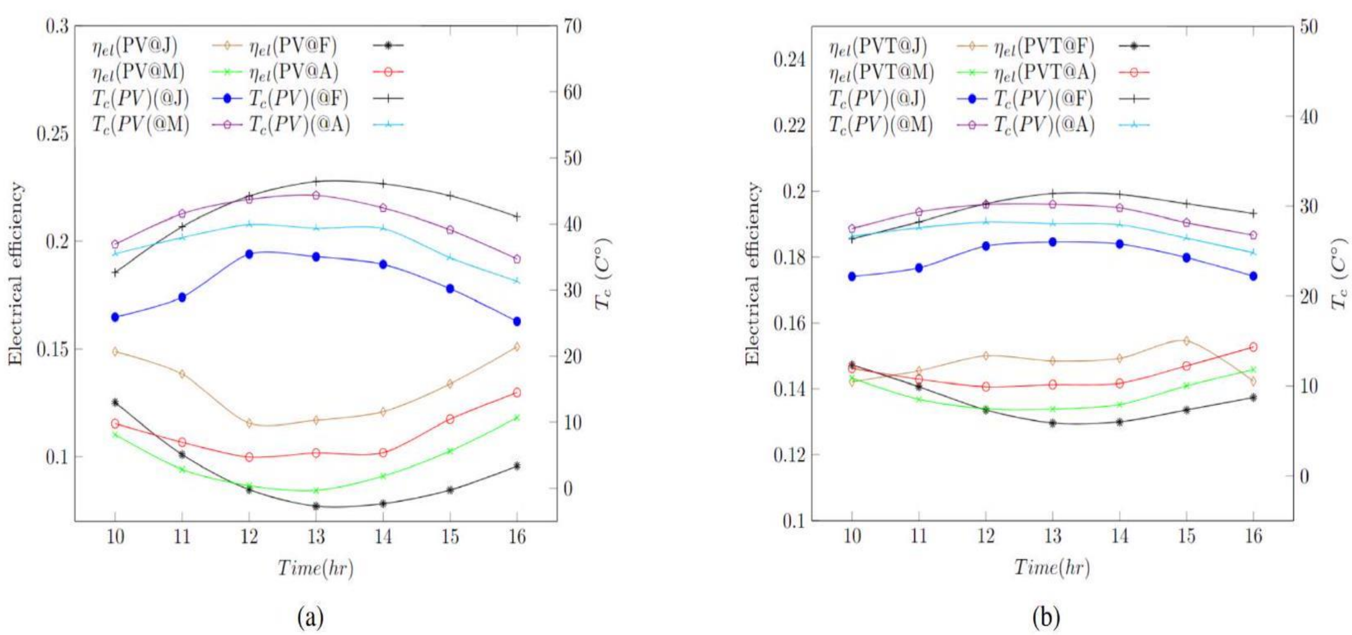

Figure 4.7: Electrical efficiency during the experimental days for: a. PV system, b. PVT system

sustainable energy solutions, solar space heating is becoming an increasingly viable option for both new constructions and retrofitted buildings. Its application not only helps reduce operational energy costs but also aligns with global efforts toward cleaner energy utilization [87][88][89]. In this framework, CFD methods were used to construct and simulate the heating of a specific space represented by a small room, thereby illustrating the impact of the current research systems on heating this space. Various programs from the Ansys package were utilized in order to create the model, perform meshing operations, simulate, acquire results, and perform post-processing processes.

4.6.1 Physical description

In this study, the designated area for heating consists of a single room measuring 4.8 m in length, 2.7 m in height, and 2.4 m in width. It comprises insulated walls, excluding the window wall, a glazed window of (2.4×1.2)m, a radiator with dimensions of (1.4 m × 0.84 x0.05)m, an intake orifice for fresh air of (0.5x0.02)m, and an exhaust orifice of (0.8x0.05) m. The physical description of the specific room is depicted in figure 4.8. It's worth nothing that Olesen and his colleagues [90]

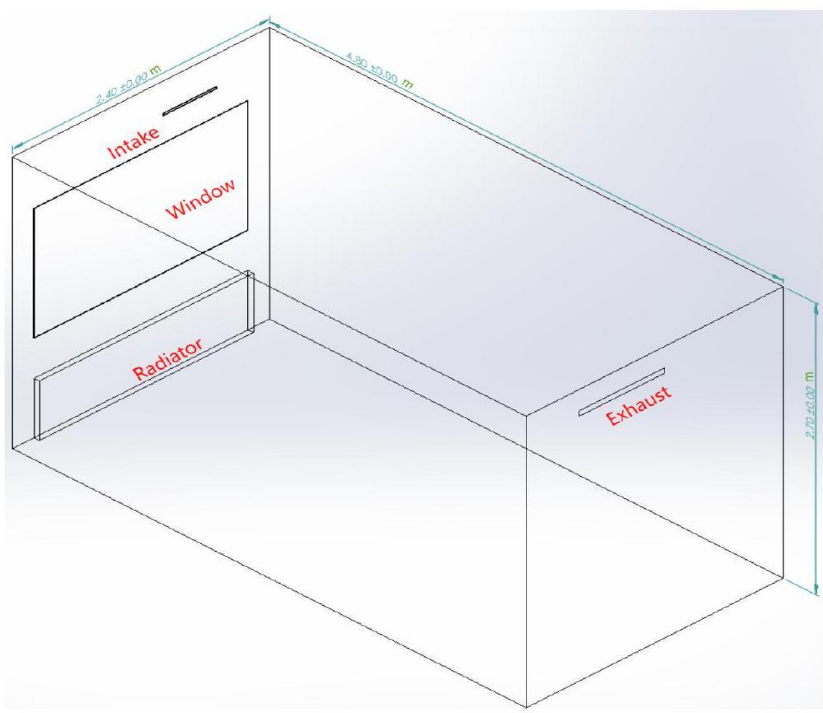

Figure 4.8: Room's physical description

previously performed experimental work research under identical room conditions; also, numerous researchers have compared their findings with his results [91][92].

4.6.2 Solver and boundary setup

Continuity, momentum, and energy equations are applied as the fundamental governing equations in this domain. These equations are utilized alongside with turbulent model $k - \epsilon$ which is considered a good model for turbulent flow prediction at low Reynolds. This model also involves the $k - \epsilon$ transport equations which consider very important equations for describing turbulent viscosity (μ_t). These equations can be described as follows [93]:

$$\frac{\partial}{\partial t}(\rho k) + \nabla \cdot (\rho k \vec{v}) = \nabla \cdot (\alpha_k \mu_{\text{eff}} \nabla k) + G_k + G_b - \rho\epsilon - Y_M + S_k \quad (4.1)$$

$$\frac{\partial}{\partial t}(\rho\epsilon) + \nabla \cdot (\rho\epsilon\vec{v}) =$$
$$\nabla \cdot (\alpha_\epsilon \mu_{\text{eff}} \nabla\epsilon) + C_{1\epsilon}\frac{\epsilon}{k}(G_k + C_{3\epsilon}G_b)$$
$$-C_{2\epsilon}\rho\frac{\epsilon^2}{k} - R_\epsilon + S_\epsilon$$

The discrete ordinates (DO) model can be employed to incorporate radiation from the heat source, and it is formulated as follows [93]:

$$\nabla(I(\vec{r},\vec{s})) + (a + \sigma_s)I(\vec{r},\vec{s}) = an^2\frac{\sigma T^4}{\pi} + \frac{\sigma_s}{4\pi}\int_0^{4\pi} I(\vec{r},\vec{s}')$$
$$\Phi(\vec{s},\vec{s}')d\Omega' \quad (4.2)$$

In this equation, the amount of radiation emitted, referred to as radiation intensity (I), is affected by several variables, including the position $\vec{r}$ and direction $\vec{s}$. Both σ_s and a denote the scattering and absorption coefficients, respectively; n represents the refractive index; The parameter σ denotes the Stefan–Boltzmann constant, ϕ represents the phase function, and Ω′ is the solid angle. The thermal balance associated with the radiator can be formulated as follows:[94]

$$\dot{m} \cdot c_p \cdot \Delta T = k \cdot A \cdot \Delta T_m \quad (4.3)$$

Hence, ΔT represents the inlet-outlet temperature differences and ΔT_m denotes the difference between the radiator's mean temperature and that of the ambient surroundings. The room's thermal comfort was depicted using a thermal indicator known as the comfort temperature, T_{comfort}. Previously, Myhren have addressed the plus sides of employing comfort temperature as compared to operative temperature [95]. Comfort temperature is a variable that is employed to determine the presumed thermal climate, similar to the more often employed operative temperature. It accounts for the balance between radiative heat transfer effects and the surrounding air temperature. It can be described as below [96]:

$$T_{\text{comfort}} = \frac{T_{\text{surface}} + (T_{\text{air}} \times u_{\text{air}})}{1 + \sqrt{(10 \times u_{\text{air}})}} \tag{4.4}$$

In this equation, T_{surface} represents the surface temperature of the radiator and $(T, u)_{\text{air}}$ indicate the temperature and velocity of the air, respectively. Various values for the supply and return water temperatures can be implemented to accommodate different system requirements, allowing for more precise control over thermal performance. By adjusting these temperatures, the system can optimize energy efficiency and ensure effective heat transfer between the water and the surrounding environment [96]. The European standard for radiators, EN 442, suggests maintaining a temperature difference of 10 K between the supply and return water temperatures to ensure optimal performance and efficiency in heating systems. This number is what the current study depended on. The following dimensionless numbers are commonly employed to describe and analyze the flow characteristics, helping to provide a clearer understanding of the fluid behavior within the system [93][94]:

1. **The Prandtl number:**

$$\text{Pr} = \frac{\nu}{\alpha} \tag{4.5}$$

This parameter indicates the relative importance of convection and conduction on a fluid and represents the kinematic viscosity to the thermal diffusivity.

2. **Reynolds number:**

$$Re = \frac{uL}{\nu} \tag{4.6}$$

Which was defined recently.

3. **Grashof number:**

$$Gr = \frac{g\beta\Delta T L^3}{\nu^2} \quad (4.7)$$

It represents the ratio of buoyant forces to viscous forces within the fluid, providing valuable insight into the dominant physical effects influencing the flow. This ratio is essential for predicting the flow behavior, as it helps determine whether the flow is more likely to be governed by buoyancy (natural convection) or by viscous forces (forced convection), which in turn influences the system's thermal and fluid dynamics. Given that the Gr/Re^2 exceeds 1, the flow was presumed to represent natural convection. To solve the complex coupling between pressure and velocity, as well as the interrelationship between the flow and energy equations, an iterative approach using the coupled scheme method was chosen. This method is well-suited for handling the simultaneous solution of the pressure and velocity fields, ensuring that the flow dynamics are accurately captured. For the discretization of the momentum and energy equations, a second-order upwind scheme was employed, which provides a more precise representation of convective terms and improves the overall accuracy of the numerical solution. In contrast, a first-order upwind scheme was used for the discretization of the turbulent kinetic energy and dissipation rate equations, balancing computational efficiency with the necessary accuracy for modeling turbulence behavior. To ensure that the numerical solution converged properly, the residuals were set within a specified range of 10^{-3} to 10^{-4} for the parameters of the equations. These residuals represent the difference between successive iterations and serve as a measure of convergence, ensuring the solution is sufficiently accurate for further analysis. The boundary conditions were defined as follows:

At the inlet:

$$T = T_i, u = u_i = 0.7 \text{ m/s}, v = w = 0$$

Where T_i represents the air temperature, and u_i is the air velocity in the x-direction. The velocity components in the y and z directions are denoted by v, and w respectively.

At the outlet: the pressure outlet condition was applied; in this way the velocity and temperature gradients at the outlet are defined as follows:

$$\frac{\partial u}{\partial x} = \frac{\partial v}{\partial x} = \frac{\partial w}{\partial x} = \frac{\partial T}{\partial x} = 0$$

For the insulated walls, adiabatic thermal conditions were applied, meaning that no heat exchange occurs through these surfaces. the heat transfer coefficient of the window wall was $0.3 w/m^2$ °C, , which defines the rate of heat transfer across the wall per unit area and temperature difference. In the current study, the radiator is modeled as having a constant source temperature, ensuring that the thermal output remains steady throughout the simulation.

.

4.6.3 Grid Independence and Model Verification

The grid independence of the model was evaluated by testing four different mesh configurations, consisting of 150,000, 385,000, 622,543, and 804,506 elements. The room temperature was calculated for each configuration to assess the impact of the mesh resolution on the solution's stability. The two highest mesh configurations exhibited strong stability and were deemed reliable for use in the model computations. Additionally, the model's validity was confirmed by comparing the simulation results with the experimental data from reference [90]. The comparison, as shown in Figure 4.9, demonstrated a good agreement between the simulated results and the referenced experimental findings, with the maximum error observed being a variation of 7.94%.

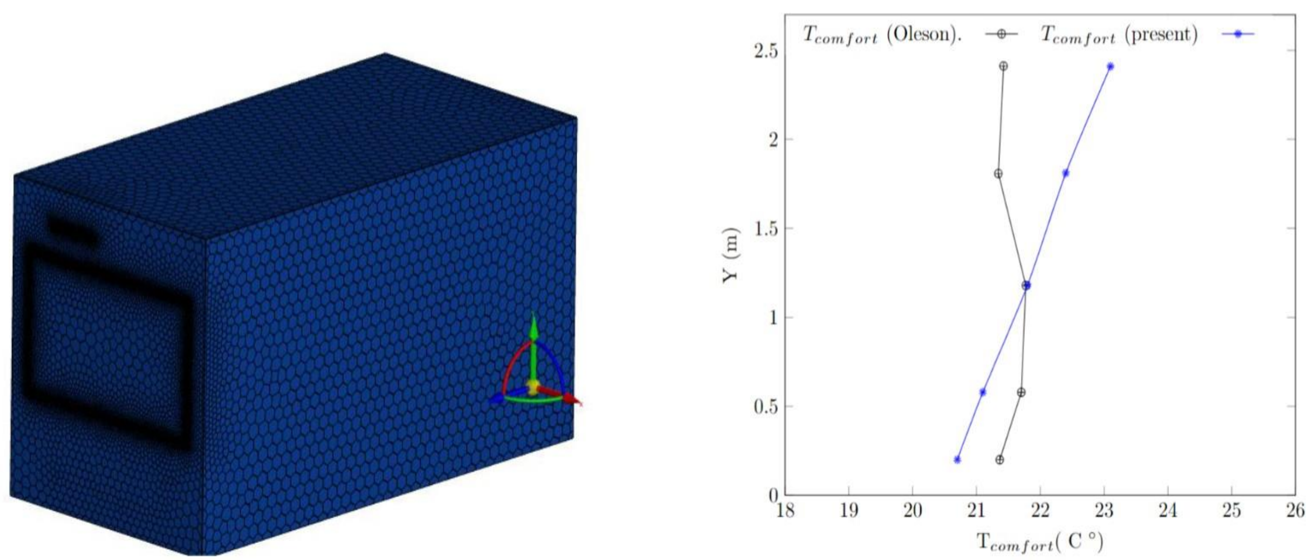

(a) (b)

Figure 4.9: a. a 3-D Mesh of the used geometry, b. Solution validation

4.6.4 Results

As previously mentioned, the main goal of the room heating simulation is to evaluate whether the ST (Solar Thermal) or PVTST (Photovoltaic Thermal Solar Thermal) system, with areas of 2 m² and 4 m², respectively, can achieve the required temperature for effectively heating a room using a water radiator. The simulation focused on analyzing the temperature distribution within a single room, where these systems were used as the primary sources of hot water to assess their performance in reaching the desired heating conditions. Figures 4.10 and 4.11 illustrate the simulation findings of the room under investigation. This figure depicts the temperature distribution in both longitudinal and cross sections. The cold airflow from the intake orifice increases progressively throughout the whole room space while simultaneously combining with the warm air emitted from the hot water radiator until it reaches the steady-state temperature. Controlling the desirable or required comfort temperature can be accomplished by installing a thermostat on the delivery side of the radiator. Figure 4.12 shows the mean room temperature data acquired throughout the course of four days during the study period using the ST and PVTST systems.

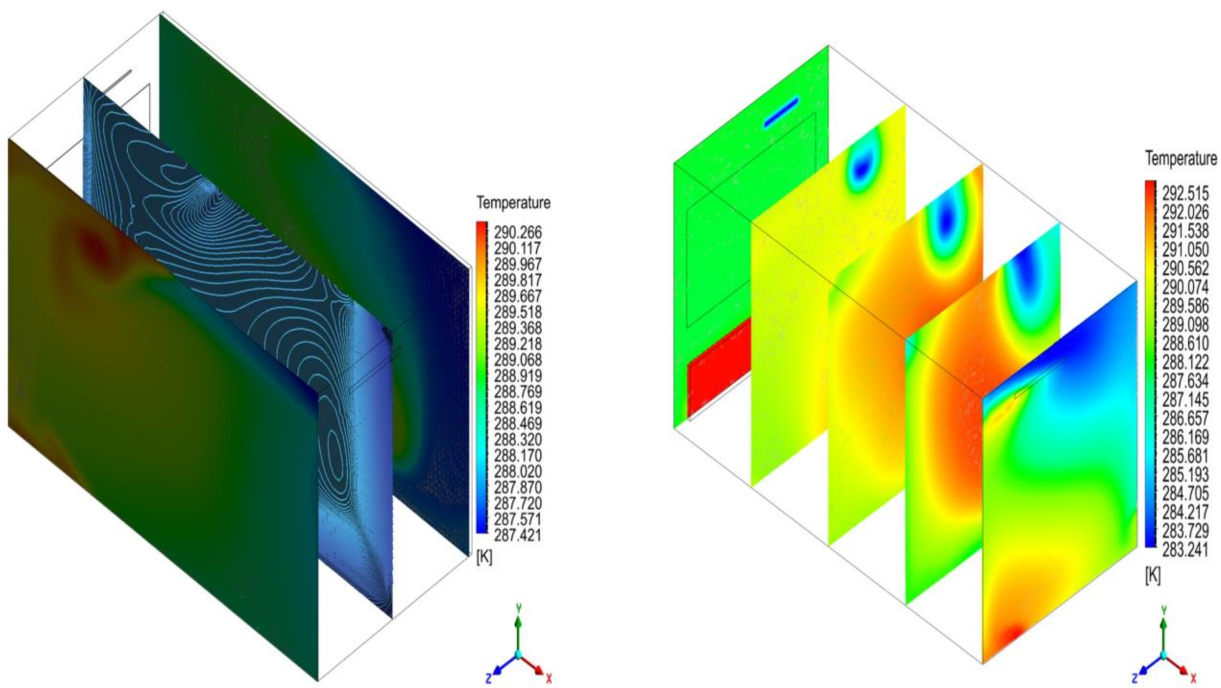

(a) (b)

Figure 4.10: Room simulation results: a. longitudinal sections, b. cross sections

This figure clearly illustrates that, over the testing period of February, March, and April, both the ST and PVTST systems are capable of providing an adequate amount of heat to effectively warm a single room, demonstrating their ability to meet the heating requirements during these months. During these three days, the room temperature exceeded the required temperature, which is defined as 22 °C [97][98]. During January, there were several instances throughout the day when the intended temperature could not be reached. The shortfall in the ST system was approximately 15.9%, while the PVTST system experienced a shortfall of 8.18%. On the four days under investigation, the average increase in room temperature when using PVTST as a hot water provider was 7.94%, 4.86%, 4.80%, and 5.05%, respectively, more than when using the ST system. In order to prevent the consumption of additional energy, a control system might control the rate of increase; however, the current study does not include an energy control system.

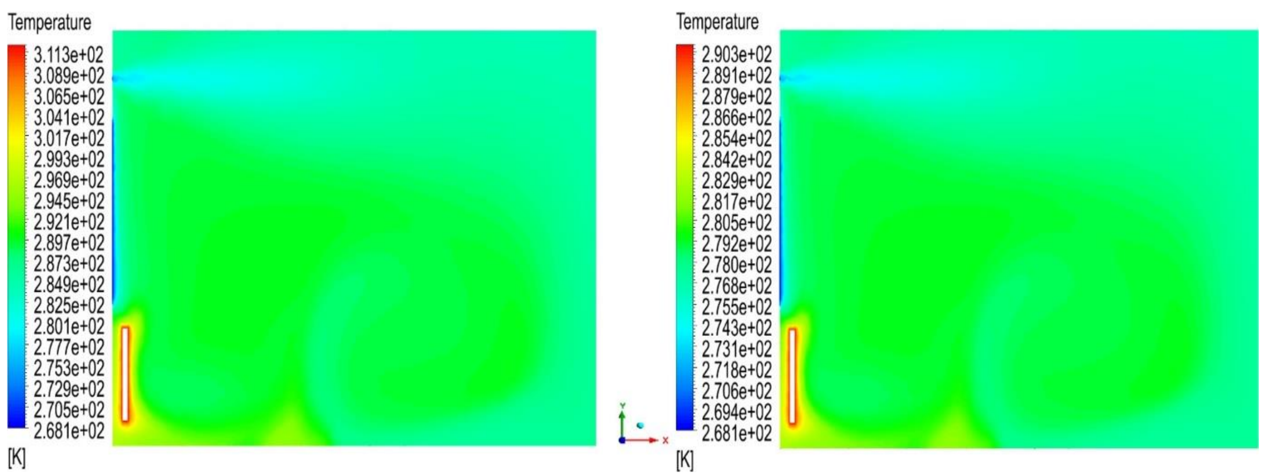

Figure 4.11: Front view of the room's simulation for: a. maximum radiator surface temperature, b. minimum radiator surface temperature

4.7 Analysis of the shortfall in Water supply temperature

This section is dedicated to assessing the capability of the PVTST system in meeting the required hot water demand at the appropriate temperature during the designated test hours across the selected days. To perform this evaluation, an analytical calculation was conducted to determine the average shortfall between the output temperature of the hot water produced by the PVTST system and the target temperature necessary for domestic hot water use. Based on previous studies, it has been established that

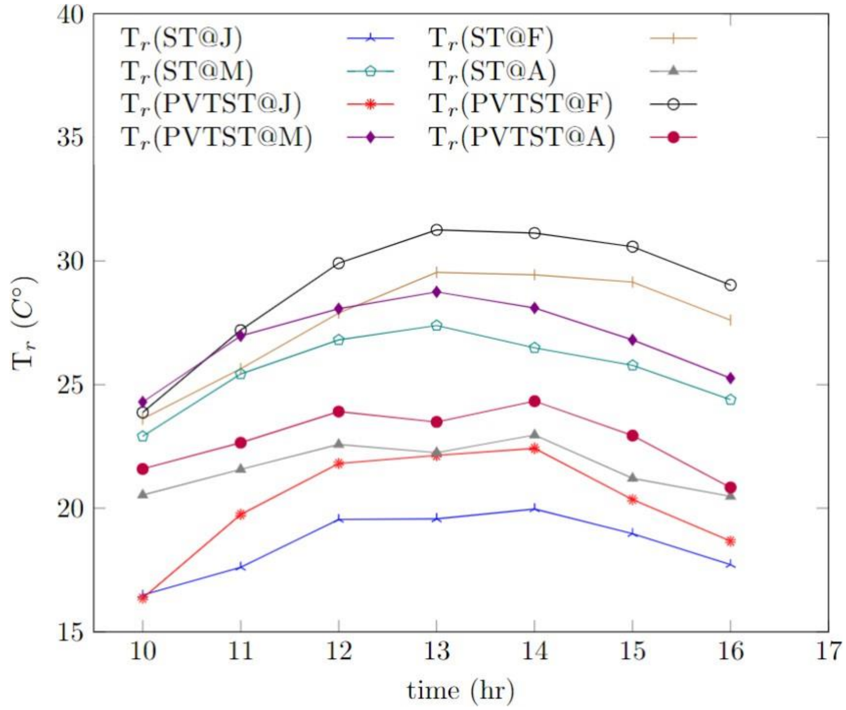

Figure 4.12: Average room temperature during the test days of the study

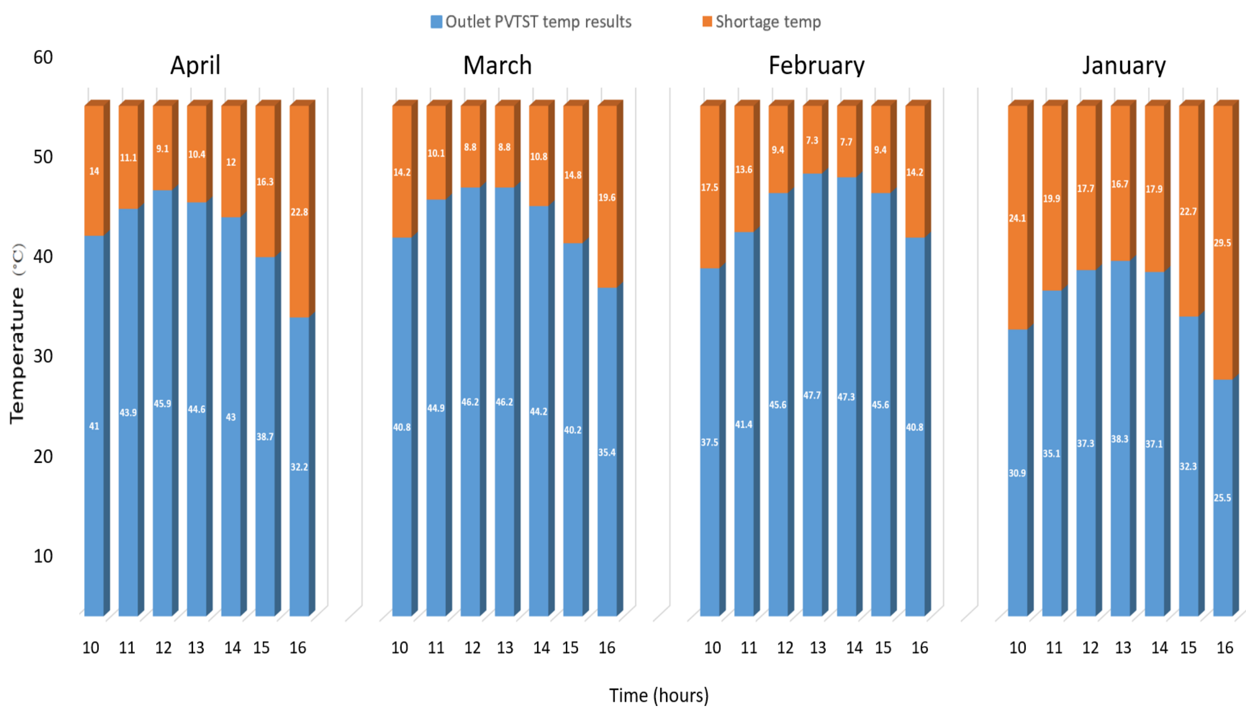

Figure 4.13: Shortfall of the supplied hot water through the study period

household hot water temperatures of 50°C [99], 55°C [100], or 60°C [101] are typically sufficient to meet the daily domestic hot water requirements. The results from the analysis show that the PVTST system can fulfill an average of 61.4% of the daily domestic hot water demand on the first test day, 79.4% on the second day, 77.3% on the third day, and 75% on the fourth day, assuming the target temperature for the hot water is set at 55°C. These percentages represent the portion of hot water demand met by the system throughout the test period, offering a glimpse into the system's efficiency and reliability.

Figure 4.13 provides a visual representation of the temperature shortfall relative to the provided hot water temperature from the PVTST system during the period from 10 a.m. to 4 p.m. across the months of January, February, March, and April. This figure clearly highlights the fluctuations in temperature shortfall during these months, showing how the system's performance varies across the test period and allowing for a better understanding of its ability to meet domestic hot water needs under different environmental conditions

Chapter 5

Conclusions & suggestions

4.1 Conclusions

The rising worldwide need for renewable energy sources has resulted in heightened interest in hybrid solar energy systems that effectively harness both electrical and thermal energy. PVT systems have evolved as an innovative technology that concurrently generates energy and recovers waste heat from PV modules. The efficiency of PVT systems can be significantly improved by integrating them with traditional solar thermal (ST) collectors, such as flat plate collectors or any other types. This integration enhances the overall thermal performance of the system, as it combines the benefits of both technologies. While the PVT system captures both heat and electricity, the addition of ST collectors allows for optimized heat absorption, thereby increasing the thermal output and efficiency of the system, particularly in situations where higher thermal energy is required.

A PVTST hybrid system combines a solar thermal collector in series with a PVT to first catch solar radiation, therefore converting some of it into electricity, and then transmits the residual heat to a working fluid. The preheated fluid then passes through the flat plate solar collector (ST) to raise its temperature even more, therefore maximizing the overall efficiency of the system. By reducing the running temperature of the PV module, this design improves thermal energy capture and simultaneously enhances its electrical efficiency.

This study experimentally assessed the performance of a PVT system integrated in series with a ST system. This study examines the heating of an individual room and demonstrates if the primary research system can generate sufficient heat. The study additionally aims to predict potential deficiencies in hot water delivery. The evaluation of the utilized systems primarily concentrated on their energy, exergy, and electrical performance metrics. The collected data was accurately calculated, analyzed, and thereafter discussed. The outcomes can be articulated as follows:

- **Energy and Temperature Boost**: The PVTST system offers an effective solution for simultaneously generating both electrical energy and increasing the temperature of the hot water produced by the traditional solar thermal (ST) system, thereby optimizing overall system performance.
- **Increase in Hot Water Temperature**: A significant increase in hot water temperature was observed when utilizing the PVTST system. Compared to the ST system, the PVTST system showed an average increase in outlet temperature of (6.15°C, 6.65°C, 7.51°C, and 5.48°C) on the four test days, respectively.
- **Energy Yield Enhancement**: The results highlighted that the energy output of the PVTST system was higher by an average of (213.71 W, 231.07 W, 265.78 W, and 190.41 W) when compared to the energy yield from the ST system on the selected

test days.

◎ **Thermal Efficiency Improvement**: The thermal efficiency of the PVTST system showed an average increase of 24.8%, 18.2%, 22.3%, and 19.4% on the four test days, respectively, when compared to the thermal efficiency of the ST collector.

◎ **Exergy Efficiency Increase**: The exergy efficiency of the PVTST system showed average increases of 7.98%, 7.45%, 7.82%, and 6.97% relative to the ST system on the four test days, respectively, indicating a more efficient conversion of thermal energy into useful work.

◎ **Electrical Efficiency Comparison**: When compared to traditional PV panels, the PVT system demonstrated significant improvements in electrical efficiency, with estimated increases of 31.04%, 41.16%, 47.34%, and 11.55% on the four test days.

◎ **Heating Sufficiency**: The ST and PVTST systems were sufficient to heat a single room on the test days of February, March, and April. However, in January, these systems were unable to meet the required heating demands, resulting in a shortfall of 15.9% for the ST system and 8.18% for the PVTST system.

◎ **Hot Water Temperature Coverage**: Throughout the test days, the PVTST system successfully met an average of 61.4%, 79.4%, 77.3%, and 75% of the required hot water temperature on the respective days, demonstrating its efficiency in fulfilling domestic hot water needs.

5.2 Suggestions and future works

The current investigation lays a strong foundation for the advancement of hybrid PVT-ST systems; however, several aspects remain open for further exploration. Future research should focus on improving the **economic feasibility**, **system sustainability**, and **overall efficiency** of these systems. For widespread deployment of PVT-ST technology, it is crucial to pursue advancements in system design, explore the use of novel materials, integrate intelligent control mechanisms, and evaluate real-world operational performance.

The performance of PVT-ST systems is influenced by numerous variables such as **solar irradiation levels**, **ambient environmental conditions**, **flow rates**, **material properties**, and **system configurations**. While earlier studies have highlighted the potential of these hybrid systems, further investigation is necessary to refine their architecture, enhance material performance, and develop smart control algorithms, as well as assess their cost-effectiveness for broader implementation.

The following future research directions are recommended:

1. System Design Optimization

- Fluid Dynamics and Energy Yield: Study the impact of different configurations on fluid flow behavior, pressure drops, and energy output.
- Advanced Heat Exchanger Configurations: Investigate the effectiveness of alternative designs, such as vortex generators, microchannels, plate-fin exchangers, and double-tube systems, to improve heat transfer from the PV surface to the working fluid.
- Surface Area Modification: Explore the effect of varying the surface areas of the PVT and ST components to maximize energy and power efficiency.
- Spatial Arrangement Optimization: Analyze the optimal distance between PVT and ST modules to reduce thermal losses and improve system integration.

2. Performance Analysis under Varying Conditions

- Geographical and Climatic Assessment: Evaluate system performance across a range of climatic zones, including arid, cold, and humid regions, to assess adaptability.
- Environmental Influences: Study the effects of wind speed, ambient temperature, humidity, and dust accumulation on the system's performance.
- Low Solar Irradiance Scenarios: Assess system effectiveness during early morning, late evening, or cloudy conditions.

- Radiation Type Analysis: Examine the influence of direct vs. diffuse solar radiation on overall energy generation.

3. Optimization of Tilt Angle and Orientation

- Inclination and Azimuth Analysis: Identify the optimal tilt angle and azimuth orientation to enhance solar energy capture.
- Static vs. Dynamic Tracking Systems: Evaluate the feasibility and energy gains of incorporating solar tracking systems for real-world applications.

4. Integration of Energy Storage Systems

- Thermal Storage Options: Incorporate water-based or phase-change material (PCM)-based thermal storage tanks to ensure a steady supply of hot water during low solar periods.
- Insulation Techniques: Analyze different tank insulation methods to minimize heat losses.
- Electrical Storage Solutions: Consider the integration of battery systems (e.g., Li-ion, flow batteries) to support the electrical component of hybrid systems.
- Energy Management Strategies: Develop algorithms for coordinated thermal and electrical load management to enhance overall efficiency and reliability.

5. Economic and Environmental Impact Assessment

- Life Cycle Cost Analysis: Evaluate the long-term operational costs and economic return of the systems.
- Scale-Based Cost-Benefit Analysis: Compare performance and costs for small-scale versus large-scale implementations.
- Carbon Footprint Estimation: Assess the environmental benefits in terms of greenhouse gas reduction and energy savings compared to conventional systems.
- Sustainable Materials: Investigate the use of recyclable and eco-friendly materials to improve the system's sustainability.
- Policy and Incentive Evaluation: Analyze how the integration of hybrid systems aligns with renewable energy regulations, government incentives, and subsidies across different countries.

6. Artificial Intelligence (AI) Integration

- Smart Monitoring and Control: Integrate AI-based control systems to facilitate automated operation, real-time performance monitoring, fault detection, and dynamic optimization of hybrid systems.

Bibliography

[1] World Resources Institute, “World Resources Institute,” 2025. Accessed: Feb. 13, 2025.

[2] M. Amir, R. G. Deshmukh, H. M. Khalid, Z. Said, A. Raza, S. Muyeen, A.-S. Nizami, R. M. Elavarasan, R. Saidur, and K. Sopian, “Energy storage technologies: An integrated survey of developments, global economical/environmental effects, optimal scheduling model, and sustainable adaption policies,” *Journal of Energy Storage*, vol. 72, p. 108694, 2023.

[3] H. K. Stranddorf, L. Hoffmann, and A. Schmidt, “Impact categories, normalisation and weighting in lca,” *Impact categories, normalisation and weighting in LCA.*, p. 2, 2005.

[4] W. D. Fletcher and C. B. Smith, *Reaching net zero: What it takes to solve the global climate crisis*. Elsevier, 2020.

[5] C. UNFCCC, “Paris agreement,” *United Nations*, 2015.

[6] L. Cumplido-Marin, A. R. Graves, P. J. Burgess, and A. Williams, “On-farm greenhouse gas emissions associated with the cultivation of two new bioenergy crops in the uk,” *Energy Nexus*, vol. 8, p. 100162, 2022.

[7] International Energy Agency, “Net Zero by 2050 Scenario,” 2021. Accessed: Feb. 13, 2025.

[8] A. Olabi, K. Elsaid, K. Obaideen, M. A. Abdelkareem, H. Rezk, T. Wilberforce, H. M. Maghrabie, and E. T. Sayed, “Renewable energy systems: Comparisons, challenges and barriers, sustainability indicators, and the contribution to un sustainable development goals,” *International Journal of Thermofluids*, vol. 20, p. 100498, 2023.

[9] K. Obaideen, M. N. AlMallahi, A. H. Alami, M. Ramadan, M. A. Abdelkareem, N. She- hata, and A. Olabi, “On the contribution of solar energy to sustainable developments goals: Case study on mohammed bin rashid al maktoum solar park,” *International Journal of Thermofluids*, vol. 12, p. 100123, 2021.

[10] N. Patel and D. Mehta, “The asymmetry effect of industrialization, financial development and globalization on co2 emissions in india,” *International Journal of Thermofluids*, vol. 20, p. 100397, 2023.

[11] A. M. Reveshti, A. Ebrahimpour, and J. Razmara, “Investigating the effect of

new and old weather data on the energy consumption of buildings affected by global warming in different climates," *International Journal of Thermofluids*, vol. 19, p. 100377, 2023.

[12] N. Wood and K. Roelich, "Tensions, capabilities, and justice in climate change mitigation of fossil fuels," *Energy Research & Social Science*, vol. 52, pp. 114–122, 2019.

[13] K. Handayani, Y. Krozer, and T. Filatova, "From fossil fuels to renewables: An analysis of long-term scenarios considering technological learning," *Energy policy*, vol. 127, pp. 134– 146, 2019.

[14] R. Jonynas, E. Puida, R. Poškas, L. Paukštaitis, H. Jouhara, J. Gudzinskas, G. Miliauskas, and V. Lukoševičius, "Renewables for district heating: The case of lithuania," *Energy*, vol. 211, p. 119064, 2020.

[15] M. Chandrasekar and T. Senthilkumar, "Five decades of evolution of solar photovoltaic thermal (pvt) technology–a critical insight on review articles," *Journal of Cleaner Production*, vol. 322, p. 128997, 2021.

[16] A. Sharif, M. S. Meo, M. A. F. Chowdhury, and K. Sohag, "Role of solar energy in reducing ecological footprints: An empirical analysis," *Journal of Cleaner Production*, vol. 292, p. 126028, 2021.

[17] M. S. Guney, "Solar power and application methods," *Renewable and Sustainable Energy Reviews*, vol. 57, pp. 776–785, 2016.

[18] I. IEA, "Tracking clean energy progress 2023," IEA Paris, France, 2023.

[19] M. Dehghanimadvar, R. Shirmohammadi, F. Ahmadi, A. Aslani, and K. R. Khalilpour, "Mapping the development of various solar thermal technologies with hype cycle analysis," *Sustainable Energy Technologies and Assessments*, vol. 53, p. 102615, 2022.

[20] B. K. Sahu, "A study on global solar pv energy developments and policies with special focus on the top ten solar pv power producing countries," *Renewable and Sustainable Energy Reviews*, vol. 43, pp. 621–634, 2015.

[21] M. C. Browne, B. Norton, and S. J. McCormack, "Heat retention of a photo-voltaic/thermal collector with pcm," *Solar Energy*, vol. 133, pp. 533–548, 2016.

[22] Y. Tripanagnostopoulos, M. Souliotis, R. Battisti, and A. Corrado, "Energy, cost and lca results of pv and hybrid pv/t solar systems," *Progress in Photovoltaics: Research and applications*, vol. 13, no. 3, pp. 235–250, 2005.

[23] T. M. Sathe and A. Dhoble, “A review on recent advancements in photovoltaic thermal techniques,” *Renewable and Sustainable Energy Reviews*, vol. 76, pp. 645–672, 2017.

[24] C. Good, J. Chen, Y. Dai, and A. G. Hestnes, “Hybrid photovoltaic-thermal systems in buildings–a review,” *Energy Procedia*, vol. 70, pp. 683–690, 2015.

[25] V. Authors, “Ñ pvt roadmap: a european guide for the development and market intro- duction of pvt technology,” 2005. Netherlands: N. p.

[26] C. Maurer, C. Cappel, and T. E. Kuhn, “Progress in building-integrated solar thermal systems,” *Solar Energy*, vol. 154, pp. 158–186, 2017.

[27] W. A. Abdelmaksoud, “Solar energy utilization for underfloor heating system in residential buildings,” *Energy Reports*, vol. 12, pp. 979–987, 2024.

[28] R. Kumar, R. Nadda, S. Kumar, K. Kumar, A. Afzal, R. A. Razak, and M. Sharifpur, “Heat transfer and friction factor correlations for an impinging air jets solar thermal collector with arc ribs on an absorber plate,” *Sustainable Energy Technologies and Assessments*, vol. 47, p. 101523, 2021.

[29] P. Rani and P. Tripathy, “Experimental investigation on heat transfer performance of solar collector with baffles and semicircular loops fins under varied air mass flow rates,” *International Journal of Thermal Sciences*, vol. 178, p. 107597, 2022.

[30] A. Hobbi and K. Siddiqui, “Experimental study on the effect of heat transfer enhancement devices in flat-plate solar collectors,” *International Journal of Heat and Mass Transfer*, vol. 52, no. 19-20, pp. 4650–4658, 2009.

[31] M. H. Alkhafaji, B. Freegah, and M. H. Alhamdo, “Study the influence of adding fins to the plate of the solar collector on thermal performance under natural phenomena,” *International Communications in Heat and Mass Transfer*, vol. 135, p. 106058, 2022.

[32] Y. Fu, Y. Xia, X. Lin, Z. Cheng, Z. Zhang, J. Feng, and H. Wang, “A novel structure design and numerical analysis of porous media-assisted enhanced thermal performance of flat-plate solar collector,” *Thermal Science and Engineering Progress*, vol. 40, p. 101777, 2023.

[33] L. S. Sundar, A. Misganaw, M. K. Singh, A. M. Pereira, and A. C. Sousa, “Efficiency, energy and economic analysis of twisted tape inserts in a thermosyphon solar flat plate collector with cu nanofluids,” *Renewable Energy Focus*, vol. 35, pp. 10–31, 2020.

[34] S. Algarni, "Evaluation and optimization of the performance and efficiency of a hybrid flat plate solar collector integrated with phase change material and heat sink," *Case Studies in Thermal Engineering*, vol. 45, p. 102892, 2023.

[35] F. A. da Silva, D. J. Dezan, A. V. Pantaleao, and L. O. Salviano, "Longitudinal vortex generator applied to heat transfer enhancement of a flat plate solar water heater," *Applied Thermal Engineering*, vol. 158, p. 113790, 2019.

[36] T. R. Desisa, "Experimental and numerical investigation of heat transfer characteristics in solar flat plate collector using nanofluids," *International Journal of Thermofluids*, vol. 18, p. 100325, 2023.

[37] A. N. Binks, S. J. Kenway, P. A. Lant, and B. W. Head, "Understanding australian household water-related energy use and identifying physical and human characteristics of major end uses," *Journal of Cleaner Production*, vol. 135, pp. 892–906, 2016.

[38] Y. Xu, J. Litardo, C. Del Pero, F. Leonforte, and P. Caputo, "District energy models: A comparative assessment of features and criteria for tools selection," *Energy and Buildings*, p. 114291, 2024.

[39] S. Murugan and B. Horák, "Tri and polygeneration systems-a review," *Renewable and Sustainable Energy Reviews*, vol. 60, pp. 1032–1051, 2016.

[40] M. Wolf, "Performance analyses of combined heating and photovoltaic power systems for residences," *Energy Conversion*, vol. 16, no. 1-2, pp. 79–90, 1976.

[41] B. Chhugani, P. Pärisch, S. Helmling, and F. Giovannetti, "Comparison of pvt-heat pump systems with reference systems for the energy supply of a single-family house," *Solar Energy Advances*, vol. 3, p. 100031, 2023.

[42] M. Qu, X. Yan, H. Wang, Y. Hei, H. Liu, and Z. Li, "Energy, exergy, economic and environmental analysis of photovoltaic/thermal integrated water source heat pump water heater," *Renewable Energy*, vol. 194, pp. 1084–1097, 2022.

[43] S. Zhu, K. Wang, I. González-Pino, J. Song, G. Yu, E. Luo, and C. N. Markides, "Techno-economic analysis of a combined heat and power system integrating hybrid photovoltaic-thermal collectors, a stirling engine and energy storage," *Energy Conversion and Management*, vol. 284, p. 116968, 2023.

[44] R. Tripathi and G. Tiwari, "Energetic and exergetic analysis of n partially covered photovoltaic thermal-compound parabolic concentrator (pvt-cpc) collectors connected in series," *Solar Energy*, vol. 137, pp. 441–451, 2016.

[45] Á. A. Bayod-Rújula, J. Uche, J. A. Tejero, A. Del Amo, A. Martínez-Gracia, S.

Usón, *et al.*, "Integration of thermoelectric generators (teg) in solar pvt panels," tech. rep., 2019.

[46] N. S. Nazri, A. Fudholi, W. Mustafa, C. H. Yen, M. Mohammad, M. H. Ruslan, and K. Sopian, "Exergy and improvement potential of hybrid photovoltaic ther- mal/thermoelectric (pvt/te) air collector," *Renewable and Sustainable Energy Reviews*, vol. 111, pp. 132–144, 2019.

[47] A. Akbar, G. Najafi, S. Gorjian, A. Kasaeian, and M. Mazlan, "Performance enhancement of a hybrid photovoltaic-thermal-thermoelectric (pvt-te) module using nanofluid-based cooling: Indoor experimental tests and multi-objective optimization," *Sustainable Energy Technologies and Assessments*, vol. 46, p. 101276, 2021.

[48] A. Salari, A. Parcheforosh, A. Hakkaki-Fard, and A. Amadeh, "A numerical study on a photovoltaic thermal system integrated with a thermoelectric generator module," *Renewable energy*, vol. 153, pp. 1261–1271, 2020.

[49] A. Alklaibi, L. S. Sundar, and A. Sousa, "Experimental analysis of exergy efficiency and entropy generation of diamond/water nanofluids flow in a thermosyphon flat plate solar collector," *International Communications in Heat and Mass Transfer*, vol. 120, p. 105057, 2021.

[50] Z. Tian, B. Perers, S. Furbo, and J. Fan, "Thermo-economic optimization of a hybrid solar district heating plant with flat plate collectors and parabolic trough collectors in series," *Energy Conversion and Management*, vol. 165, pp. 92–101, 2018.

[51] J. F. Rosales-Pérez, A. Villarruel-Jaramillo, M. Pérez-García, J. M. Cardemil, and R. Escobar, "Techno-economic analysis of hybrid solar thermal systems with flat plate and parabolic trough collectors in industrial applications," *Alexandria Engineering Journal*, vol. 86, pp. 98–119, 2024.

[52] S. Algarni and K. Irshad, "Performance evaluation of a hybrid thermoelectric generator and flat plate solar collector system in a semi-arid climate," *Case Studies in Thermal Engineering*, vol. 44, p. 102842, 2023.

[53] F. A. Boyaghchi, M. Chavoshi, and V. Sabeti, "Optimization of a novel combined cooling, heating and power cycle driven by geothermal and solar energies using the water/cuo (copper oxide) nanofluid," *Energy*, vol. 91, pp. 685–699, 2015.

[54] F. A. Boyaghchi and M. Chavoshi, "Multi-criteria optimization of a micro solar-geothermal cchp system applying water/cuo nanofluid based on exergy,

exergoeconomic and exer- goenvironmental concepts," *Applied Thermal Engineering*, vol. 112, pp. 660–675, 2017.

[55] A. Buonomano, F. Calise, A. Palombo, and M. Vicidomini, "Energy and economic analysis of geothermal–solar trigeneration systems: A case study for a hotel building in ischia," *Applied Energy*, vol. 138, pp. 224–241, 2015.

[56] L. F. Fuentes-Cortés, A. W. Dowling, C. Rubio-Maya, V. M. Zavala, and J. M. Ponce- Ortega, "Integrated design and control of multigeneration systems for building complexes," *Energy*, vol. 116, pp. 1403–1416, 2016.

[57] S. Hands, S. Sethuvenkatraman, M. Peristy, D. Rowe, and S. White, "Performance analysis & energy benefits of a desiccant based solar assisted trigeneration system in a building," *Renewable Energy*, vol. 85, pp. 865–879, 2016.

[58] S. Soutullo, L. Bujedo, J. Samaniego, D. Borge, J. Ferrer, R. Carazo, and M. Heras, "Energy performance assessment of a polygeneration plant in different weather conditions through simulation tools," *Energy and Buildings*, vol. 124, pp. 7–18, 2016.

[59] T. Ma, M. Li, and A. Kazemian, "Photovoltaic thermal module and solar thermal collector connected in series to produce electricity and high-grade heat simultaneously," *Applied Energy*, vol. 261, p. 114380, 2020.

[60] M. Li, D. Zhong, T. Ma, A. Kazemian, and W. Gu, "Photovoltaic thermal module and solar thermal collector connected in series: Energy and exergy analysis," *Energy Conversion and Management*, vol. 206, p. 112479, 2020.

[61] A. Kazemian, A. Parcheforosh, A. Salari, and T. Ma, "Optimization of a novel photovoltaic thermal module in series with a solar collector using taguchi based grey relational analysis," *Solar Energy*, vol. 215, pp. 492–507, 2021.

[62] Z. Han, K. Liu, G. Li, X. Zhao, and S. Shittu, "Electrical and thermal performance comparison between pvt-st and pv-st systems," *Energy*, vol. 237, p. 121589, 2021.

[63] V. Suresh, S. M. Iqbal, K. Reddy, B. Pesala, *et al.*, "3-d numerical modelling and experimental investigation of coupled photovoltaic thermal and flat plate collector," *Solar Energy*, vol. 224, pp. 195–209, 2021.

[64] A. Kazemian, A. Salari, T. Ma, and H. Lu, "Application of hybrid nanofluids in a novel combined photovoltaic/thermal and solar collector system," *Solar Energy*, vol. 239, pp. 102–116, 2022.

[65] A. H. Alikhan, M. Kazemi, and H. Soroush, “Enhanced performance of photovoltaic ther- mal module and solar thermal flat plate collector connected in series through integration with phase change materials: A comparative study,” *Thermal Science and Engineering Progress*, vol. 47, p. 102305, 2024.

[66] O. M. Hamdoon, O. R. Alomar, and B. M. Salim, “Performance analysis of hybrid photovoltaic thermal solar system in iraq climate condition,” *Thermal Science and Engineering Progress*, vol. 17, p. 100359, 2020.

[67] R. Liang, J. Zhang, and C. Zhou, “Dynamic simulation of a novel solar heating system based on hybrid photovoltaic/thermal collectors (pvt),” *Procedia Engineering*, vol. 121,pp. 675–683, 2015.

[68] J. Glembin, T. Haselhorst, J. Steinweg, and G. Rockendorf, “Simulation and evaluation of solar thermal combi systems with direct integration of solar heat into the space heating loop,” *Energy Procedia*, vol. 91, pp. 450–459, 2016.

[69] M. Herrando, C. N. Markides, and K. Hellgardt, “A uk-based assessment

[70] of hybrid pv and solar-thermal systems for domestic heating and power: System performance,” *Applied Energy*, vol. 122, pp. 288–309, 2014.

[71] J. Lu and G. He, “Solar seasonal storage water heating system for space heating of a house in hangzhou: Simulation using trnsys,” in *Proceedings of the 11th International Symposium on Heating, Ventilation and Air Conditioning (ISHVAC 2019) Volume III: Buildings and Energy 11*, pp. 1065–1072, Springer, 2020.

[72] A. Ahmadi, M. Ehyaei, A. Doustgani, M. E. H. Assad, A. Hmida, D. Jamali, R. Kumar, Z. Li, and A. Razmjoo, “Recent residential applications of low-temperature solar collector,” *Journal of Cleaner Production*, vol. 279, p. 123549, 2021.

[73] W. Streicher, “Solar thermal technologies for domestic hot water preparation and space heating,” in *Renewable Heating and cooling*, pp. 9–39, Elsevier, 2016.

[74] A. Kang, I. Korolija, and D. Rovas, “Photovoltaic thermal district heating: A review of the current status, opportunities and prospects,” *Applied Thermal Engineering*, vol. 217, p. 119051, 2022.

[75] A. Baggenstos, A. Mellor, A. Gagliano, C. Corino, D. Zenhäusern, D. Cabral, G. Ryan, I. Guedea, L. Brottier, U. Ruoff, *et al.*, “Existing pvt systems and solutions,” 2020.

[76] C. D'Bastiani, D. Kennedy, and A. Reynolds, "Cfd simulation of anaerobic granular sludge reactors: A review," *Water Research*, vol. 242, p. 120220, 2023.

[77] A. Z. Sheshpoli, O. Jahanian, K. Nikzadfar, and M. A. Delavar, "Numerical and experi- mental investigation on the performance of hybrid pv/thermal systems in the north of iran," *Solar Energy*, vol. 215, pp. 108–120, 2021.

[78] F. P. Incropera, D. P. DeWitt, T. L. Bergman, A. S. Lavine, *et al.*, *Fundamentals of heat and mass transfer*, vol. 6. Wiley New York, 1996.

[79] S. Sreekumar, N. Shah, J. D. Mondol, N. Hewitt, and S. Chakrabarti, "Numerical investigation and feasibility study on mxene/water nanofluid based photovoltaic/thermal system," *Cleaner Energy Systems*, vol. 2, p. 100010, 2022.

[80] S. Dubey, J. N. Sarvaiya, and B. Seshadri, "Temperature dependent photovoltaic (pv) efficiency and its effect on pv production in the world–a review," *Energy procedia*, vol. 33, pp. 311–321, 2013.

[81] M. D. Bazilian and D. Prasad, "Modelling of a photovoltaic heat recovery system and its role in a design decision support tool for building professionals," *Renewable energy*, vol. 27, no. 1, pp. 57–68, 2002.

[82] K. Y. Wenceslas and T. Ghislain, "Experimental validation of exergy optimization of a flat-plate solar collector in a thermosyphon solar water heater," *Arabian journal for Science and Engineering*, vol. 44, no. 3, pp. 2535–2549, 2019.

[83] F. Vahidinia and H. Khorasanizadeh, "Comparative energy, exergy and entropy generation study of a minichannel and a conventional solar flat plat collectors," *Energy*, vol. 304, p. 132232, 2024.

[84] A. Bejan, D. Kearney, and F. Kreith, "Second law analysis and synthesis of solar collector systems," 1981.

[85] A. E. Gürel, Ü. Ağbulut, H. Bakır, A. Ergün, and G. Yıldız, "A state of art review on estimation of solar radiation with various models," *Heliyon*, vol. 9, no. 2, 2023.

[86] H. B. Yıldırım, A. Teke, and F. Antonanzas-Torres, "Evaluation of classical parametric models for estimating solar radiation in the eastern mediterranean region of turkey," Renewable and Sustainable Energy Reviews, vol. 82, pp. 2053–2065, 2018.

[87] S. A. Kalogirou, Solar Energy Engineering: Processes and Systems. Burlington, MA:Academic Press, 2nd ed., 2013.

[88] J. A. Duffie and W. A. Beckman, Solar Engineering of Thermal Processes. Hoboken, NJ: Wiley, 4th ed., 2013.

[89] H. P. Garg and J. Prakash, Solar Energy: Fundamentals and Applications. New Delhi, India: Tata McGraw-Hill, 1st ed., 2000.

[90] B. W. Olesen, E. Mortensen, J. Thorshauge, et al., "Thermal comfort in a room heated by different methods," 1980.

[91] G. A. Ganesh, S. L. Sinha, and T. N. Verma, "Numerical simulation for optimization of the indoor environment of an occupied office building using double-panel and ventilation radiator," Journal of Building Engineering, vol. 29, p. 101139, 2020.

[92] K. Horikiri, Y. Yao, and J. Yao, "Numerical optimisation of thermal comfort improvement for indoor environment with occupants and furniture," Energy and Buildings, vol. 88, pp. 303–315, 2015.

[93] K. Horikiri, Y. Yao, and J. Yao, "Modelling conjugate flow and heat transfer in a ventilated room for indoor thermal comfort assessment," Building and Environment, vol. 77, pp. 135–147, 2014.

[94] J. A. Myhren and S. Holmberg, "Design considerations with ventilation-radiators: Comparisons to traditional two-panel radiators," Energy and buildings, vol. 41, no. 1, pp. 92–100, 2009.

[95] J. A. Myhren and S. Holmberg, "Comfort temperatures and operative temperatures in an office with different heating methods," in Proceedings of the Healthy Buildings, vol. 2, pp. 47–52, 2006.

[96] A. Ploskić, Q. Wang, and S. Sadrizadeh, "Mapping relevant parameters for efficient operation of low-temperature heating systems in nordic single-family dwellings," Applied Sciences, vol. 8, no. 10, p. 1973, 2018.

[97] A. Standard, "Thermal environmental conditions for human occupancy," ANSI/ASHRAE, 55, vol. 5, 1992.

[98] C. Liu, Z. Wang, Y. Yang, F. Zhou, L. Duanmu, Y. Zhai, Z. Lian, B. Cao, Y. Zhang, X. Zhou, et al., "A method for setting room temperature of district heating in northern china based on local thermal comfort," Applied Thermal Engineering, p. 123840, 2024.

[99] E. S. T. England, “Measurement of domestic hot water consumption indwellings,”Monitoring/Housing.professionals/Publications/Home (England), 2008.

[100] K. Ahmed, P. Pylsy, and J. Kurnitski, “Monthly domestic hot water profiles for energy calculation in finnish apartment buildings,” Energy and Buildings, vol. 97, pp. 77–85, 2015.

[101] M. Baneshi and S. A. Bahreini, “Impacts of hot water consumption pattern on optimum sizing and techno-economic aspects of residential hybrid solar water heating systems,” Sustainable Energy Technologies and Assessments, vol. 30, pp. 139–149, 2018.

Published papers:

1: 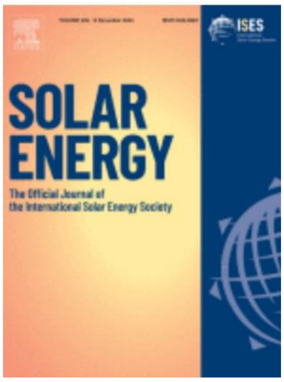

Hayder Altharwanee, David Vera, Francisco **Jurado,** ‹‹ **Experimental study on the performance of the photovoltaic thermal (PVT) connected in series with flat plate solar collector (ST)**›› Solar energy Volume 283, 113010, 15 November 2024, https://doi.org/10.1016/j.solener.2024.113010

2: 

Hayder Altharwanee, David Vera, Francisco **Jurado,** ‹‹ PV/T water-based cooling in hot climate conditions by using semi-circle baffles ›› International Journal of Power Electronics and Drive Systems (IJPEDS) Volume 15, No. 4, December 2024, pp. 2660~2673, ISSN: 2088-8694, http://doi.org/10.11591/ijpeds.v15.i4.pp2660-2673

CurriculumVitae:

Hayder Altharwanee is a pre-doctoral researcher (PhD candidate) in the Renewable Energies doctoral program at Jaén University. He achieved a bachelor's degree in mechanical engineering in 2006 from the University of Babylon in Iraq, and a master's degree in mechanical engineering \ energy conversion in 2017 from Ferdowsi Mashhad University in Iran. Presently occupying the position of Chief Engineer in the project management section of the Holy Karbala Governorate. Additionally, the individual serves as the head of the mechanical committee for the current construction of the Holy Karbala Governorate building. He has overseen various mechanical engineering projects, mostly concentrating on infrastructure development and water and sewage initiatives. His primary position entails supervising the mechanical aspects of supplying and implementing vehicles, lifting equipment, chillers, and various forms of air conditioning systems. Furthermore, he played a pivotal role as a leading member of the technical committee for several engineering projects in Karbala, directing them to esteemed businesses and guaranteeing thorough assessment of project ideas. His current study focuses on improving the thermal and electrical efficiency of the combined system (PVTST). In the meantime, he has produced three publications in international peer-reviewed journals included in the Journal Citation Reports (JCR), focusing on renewable energy.